WESTINGHOUSE CLASS 3
CUSTOMER DESIGNATED DISTRIBUTION

WCAP-10102

ANALYSIS OF CAPSULE P FROM NORTHERN STATES POWER COMPANY PRAIRIE ISLAND UNIT 1 REACTOR VESSEL RADIATION SURVEILLANCE PROGRAM

S. E. Yanichko
K. C. Tran
W. T. Kaiser

MAY 1982

Work performed under Shop Order No. ELEP 949

APPROVED: T R Mager
T. R. Mager, Manager
Metallurgical and NDE Analysis

Prepared by Westinghouse for Northern States Power Company

WESTINGHOUSE ELECTRIC CORPORATION
Nuclear Energy Systems
P.O. Box 355
Pittsburgh, Pennsylvania 15230

TABLE OF CONTENTS

LIST OF ILLUSTRATIONS

LIST OF ILLUSTRATIONS (cont)

LIST OF TABLES

LIST OF TABLES (cont)

SECTION 1
SUMMARY OF RESULTS

The analysis of the reactor vessel material contained in Capsule P, the second surveillance capsule removed from the Prairie Island Unit 1 reactor pressure vessel, led to the following conclusion:

- The capsule received an average fast-neutron fluence of 1.25×10^{19} n/cm^2 (E > 1.0 Mev) compared to a calculated value of 1.21×10^{19} n/cm^2.

- Based on the fluence measurements for Capsule P, the vessel inner surface fluence after 4.6 effective-full-power years of operation is 6.44×10^{18} n/cm^2 compared to a calculated fluence of 6.23×10^{18} n/cm^2.

- The fast-neutron fluence of 1.25×10^{19} n/cm^2 resulted in the following increases in transition temperature and decreases in upper shelf energy for the various reactor vessel surveillance materials: (see table 5-4).

Material	**50 Ft lb Temperature Increase (°F)**	**30 Ft lb Temperature Increase (°F)**	**Shelf Energy Decrease (ft lb)**
Forging C (Tangential)	25	20	7
Forging C (Axial)	51	37	16
Weld Metal	60	42	+4.5
HAZ Metal	65	70	68

- The results of the material surveillance tests indicate that the reactor pressure vessels beltline material is not very sensitive to radiation.

- The projected end-of-life fluences at various locations through the vessel wall are as follows:

Vessel Wall Location	Fast Neutron Fluence (n/cm^2) Measured	Calculated
Inner Surface	4.17×10^{19}	4.30×10^{19}
1/4 Thickness	2.78×10^{19}	2.87×10^{19}
3/4 Thickness	8.19×10^{18}	8.46×10^{18}

SECTION 2
INTRODUCTION

This report presents the results of the examination of Capsule P, the second capsule of the continuing surveillance program which monitors the effects of neutron irradiation on the Northern States Power Company, Prairie Island Unit 1 reactor pressure vessel materials under actual operating conditions.

The surveillance program for the Prairie Island Unit 1 reactor pressure vessel materials was designed and recommended by the Westinghouse Electric Corporation. A descripton of the surveillance program and the preirradiation mechanical properties of the reactor vessel materials are presented in WCAP-8086.[1] The surveillance program was planned to cover the 40-year life of the reactor pressure vessel and is based on ASTM E-185-73, "Recommended Practice for Surveillance Tests for Nuclear Reactor Vessels."[2] Westinghouse Nuclear Energy Systems personnel were contracted for the preparation of procedures for removing the first capsule from the reactor and its shipment to the Westinghouse Research and Development Laboratory, where the postirradiation mechanical testing of the Charpy V-notch impact and tensile surveillance specimens was performed.

This report summarizes testing and the postirradiation data obtained from the second material surveillance capsule (Capsule P) removed from the Prairie Island Unit 1 reactor vessel and discusses the analysis of these data. The data are also compared to results of the previously removed Prairie Island Unit 1 surveillance Capsule V reported by Davidson.[3] Using current methods,[4] heatup and cooldown pressure-temperature operating limits are established for the nuclear power plant. The heatup and cooldown pressure-temperature operating limits are presented in Appendix A.

SECTION 3
BACKGROUND

The ability of the large steel pressure vessel containing the reactor core and its primary coolant to resist fracture constitutes an important factor in ensuring safety in the nuclear industry. The beltline region of the reactor pressure vessel is the most critical region of the vessel because it is subjected to significant fast neutron bombardment. The overall effects of fast neutron irradiation on the mechanical properties of low alloy ferritic pressure vessel steels such as SA508 Class 3 (base material of Unit 1 reactor pressure vessel beltline) are well documented in the literature. Generally, low alloy ferritic materials show an increase in hardness and tensile properties and a decrease in ductility and toughness under certain conditions of irradiation.

A method for performing analyses to guard against fast fracture in reactor pressure vessels has been presented in "Protection Against Non-ductile Failure," appendix G to section III of the ASME Boiler and Pressure Vessel Code. The method utilizes fracture mechanics concepts and is based on the reference nil-ductility temperature, RT_{NDT}.

RT_{NDT} is defined as the greater of either the drop weight nil-ductility transition temperature (NDTT per ASTM E-208) or the temperature 60° F less than the 50 ft lb (and 35 mils lateral expansion) temperature as determined from Charpy specimens oriented normal to the major working direction of the material. The RT_{NDT} of a given material is used to index that material to a reference stress intensity factor curve (K_{IR} curve) which appears in appendix G of the ASME Code. The K_{IR} curve is a lower bound of dynamic, crack arrest, and static fracture toughness results obtained from several heats of pressure vessel steel. When a given material is indexed to the K_{IR} curve, allowable stress intensity factors can be obtained for this material as a function of temperature. Allowable operating limits can then be determined utilizing these allowable stress intensity factors.

RT_{NDT}, and in turn the operating limits of nuclear power plants, can be adjusted to account for the effects of radiation on the reactor vessel material properties. The radiation embrittlement or changes in mechanical properties of a given reactor pressure vessel steel can be monitored by a reactor surveillance program such as the Northern States Power Company, Prairie Island Unit 1 Reactor Vessel Radiation Surveillance Program,[1] in which a surveillance capsule is periodically removed from the operating nuclear reactor and the encapsulated specimens are tested. The increase in the Charpy V-notch 50 ft lb temperature (ΔRT_{NDT}) due to irradiation is added to the original RT_{NDT} to adjust the RT_{NDT} for radiation embrittlement. This adjusted RT_{NDT} (RT_{NDT} initial $+ \Delta RT_{NDT}$) is used to index the material to the K_{IR} curve and in turn to set operating limits for the nuclear power plant which take into account the effects of irradiation on the reactor vessel materials.

SECTION 4
DESCRIPTION OF PROGRAM

Six surveillance capsules for monitoring the effects of neutron exposure on the Prairie Island Unit 1 reactor pressure vessel core region material were inserted in the reactor vessel prior to initial plant startup. The six capsules were positioned in the reactor vessel between the thermal shield and the vessel wall at locations shown in Figure 4-1. The vertical center of the capsules is opposite the vertical center of the core.

Capsule P was removed after approximately 4.6 EFPY of plant operation. This capsule contained Charpy V-notch impact, tensile, and wedge opening loading (WOL) fracture mechanics specimens from the intermediate shell ring forging (heat 21918/38566), weld metal from the core region of the reactor vessel, and Charpy V-notch specimens from weld heat-affected zone (HAZ) material. The capsule also contained Charpy V-notch specimens from the 12-inch-thick correlation monitor material (A533 Grade B Class 1) furnished by Oak Ridge National Laboratory. The chemistry and heat treatment of the surveillance material is presented in Tables 4-1 and 4-2.

All test specimens were machined from the ¼-thickness location of the forging. Test specimens represent material taken at least one forging thickness from the quenched end of the forging. All base metal Charpy V-notch and tensile specimens were oriented with the longitudinal axis of the specimen both normal to and parallel to the principal working (hoop) direction of the forging. The WOL test specimens were machined such that the simulated crack of the specimen would propagate normal to (tangential specimens) and parallel to (axial specimens) the hoop direction of the forging. All specimens were fatigue precracked per ASTM E399-70T.

Charpy V-notch specimens from the weld metal chamfer region were oriented with the longitudinal axis of the specimens transverse to the weld direction. Tensile specimens were oriented with the longitudinal axis of the specimen parallel to the weld. Table 4-3 lists the weld procedure and information associated with the Prairie Island Unit 1 core region weldments. Capsule contained dosimeter wires of pure copper, iron, nickel, and aluminum-0.15 wt%-cobalt (cadmium-shielded and unshielded). In addition, cadmium-shielded dosimeters of Np^{237} and U^{238} were contained in the capsule and located as shown in Figure 4-2.

Thermal monitors made from two low melting eutectic alloys and sealed in Pyrex tubes were included in the capsule and were located as shown in Figure 4-2. The two eutectic alloys and their melting points are:

2.5% Ag, 97.5% Pb	Melting Point 579° F
1.75% Ag, 0.75% Sn, 97.5% Pb	Melting Point 590° F

TABLE 4-1

CHEMISTRY AND HEAT TREATMENT OF MATERIAL REPRESENTING THE CORE REGION SHELL FORGING AND WELD METAL FROM THE PRAIRIE ISLAND UNIT 1 REACTOR VESSEL

Chemical Analyses (Percent)		
Element	Intermediate Shell C 21918/38566	Weld Metal
C	0.17	0.052
Mn	1.41	1.30
P	0.013	0.017
S	0.005	0.014
Si	0.28	0.36
Ni	0.72	——
Cr	0.17	0.015
V	<0.002	0.001
Mo	0.48	0.51
Co	0.010	0.001
Cu	0.06	0.13
Sn	0.007	0.007
Zn	0.001	0.001[a]
Al	0.033	0.015
N_2	0.006	0.014
Ti	0.001[a]	0.001
Sb	0.001[a]	0.001
As	0.001[a]	0.061
B	0.003[a]	0.003[a]
Zr	0.001[a]	0.001

Heat Treatment	
Forging C Ht. No. 21918/38566	Heated at 1652/1715°F for 5 hours, water-quenched; tempered at 1175/1238°F for 5 hours, furnace-cooled; heated at 1652/1724°F for 5½ hours, water-quenched; tempered at 1202/1238°F for 5 hours, furnace-cooled; stress-relieved at 1022°F for 8 hours, furnace-cooled; stress-relieved at 1112°F for 14 hours, furnace-cooled
Weldment	Stress-relieved at 1022°F for 5 hours, furnace-cooled; stress-relieved at 1112°F for 7 hours, furnace-cooled

a. Not Detected. The number indicates the minimum limit of detection.

TABLE 4-2

CHEMISTRY AND HEAT TREATMENT OF SURVEILLANCE MATERIAL REPRESENTING 12-INCH-THICK A533 GRADE B CLASS 1 CORRELATION MONITOR MATERIAL

Chemical Analysis								
	C	Mn	P	S	Si	Ni	Mo	Cu
Ladle	0.22	1.45	0.011	0.019	0.22	0.62	0.53	——
Check	0.22	1.48	0.012	0.018	0.25	0.68	0.52	0.14
Heat Treatment								
1675 ± 25°F — 4 hours — Air-cooled 1600 ± 25°F — 4 hours — Water-quenched 1125 ± 25°F — 4 hours — Furnace-cooled 1150 ± 25°F — 40 hours — Furnace-cooled to 600°F								

TABLE 4-3

WELDING PROCEDURE AND ASSOCIATED INFORMATION FOR THE PRAIRIE ISLAND UNIT 1 CORE REGION WELDMENTS[a]

Top and Bottom of Chamfer —	Automatic submerged arc welding with multiple passes. Preheat of 356°F. Four passes on each side of chamfer. Wire: UM 40 — 2.5 mm dia. — lot: 3049 Flux: UM 89 lot: 1230 Welding Speed: 36 cm/min
Chamfer Filling —	Automatic submerged arc welding with multiple passes. Preheat of 356°F. Wire: UM 40 — 4 mm dia. — lot: 1752 Flux: UM 89 lot: 1230 Welding Speed: 40 cm/min

a. Weld Groove — Double U Configuration

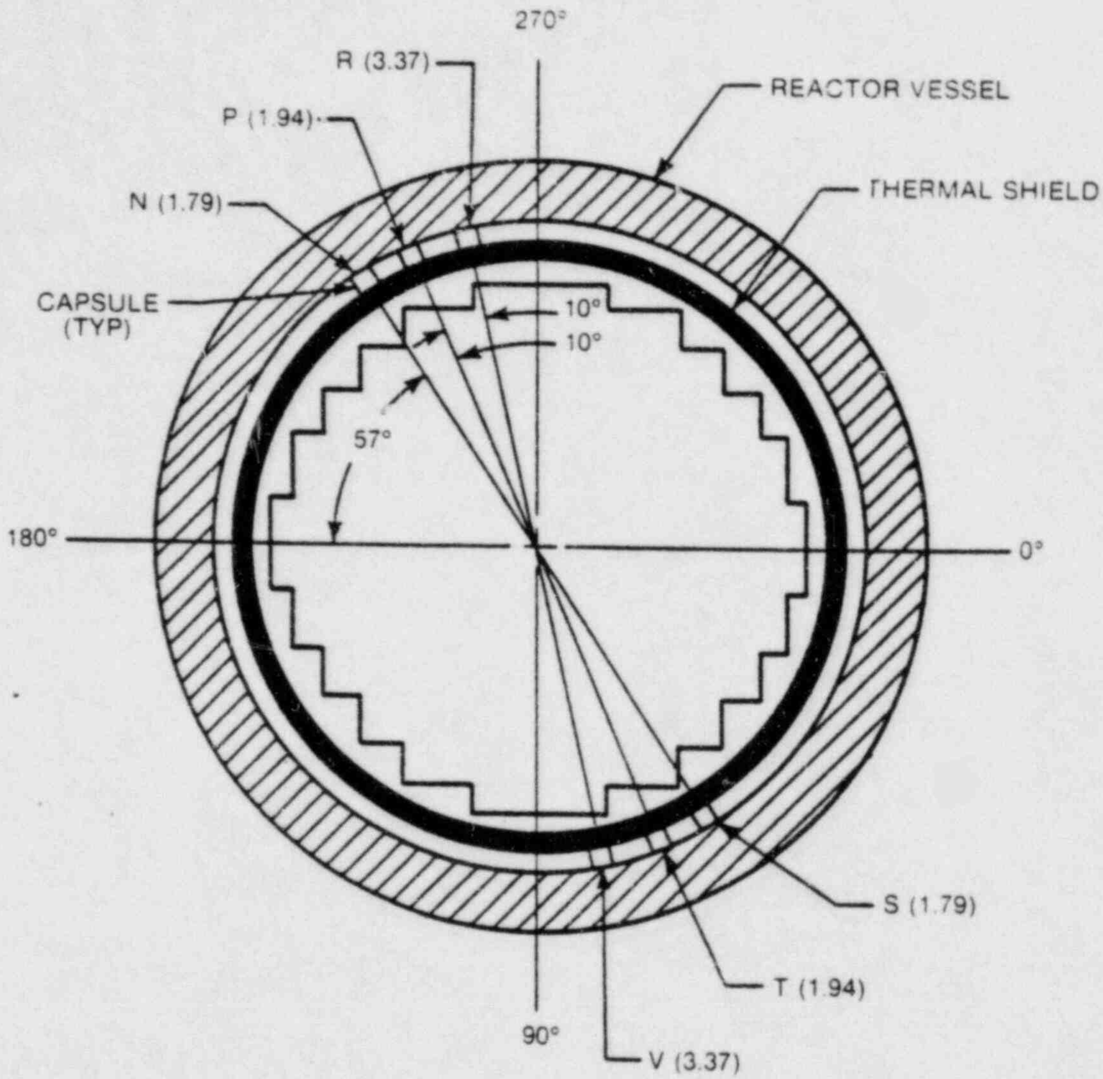

Figure 4-1. **Arrangement of Surveillance Capsules in the Prairie Island Unit 1 Reactor Vessel (Updated Lead Factors for the Capsules are Shown in Parentheses)**

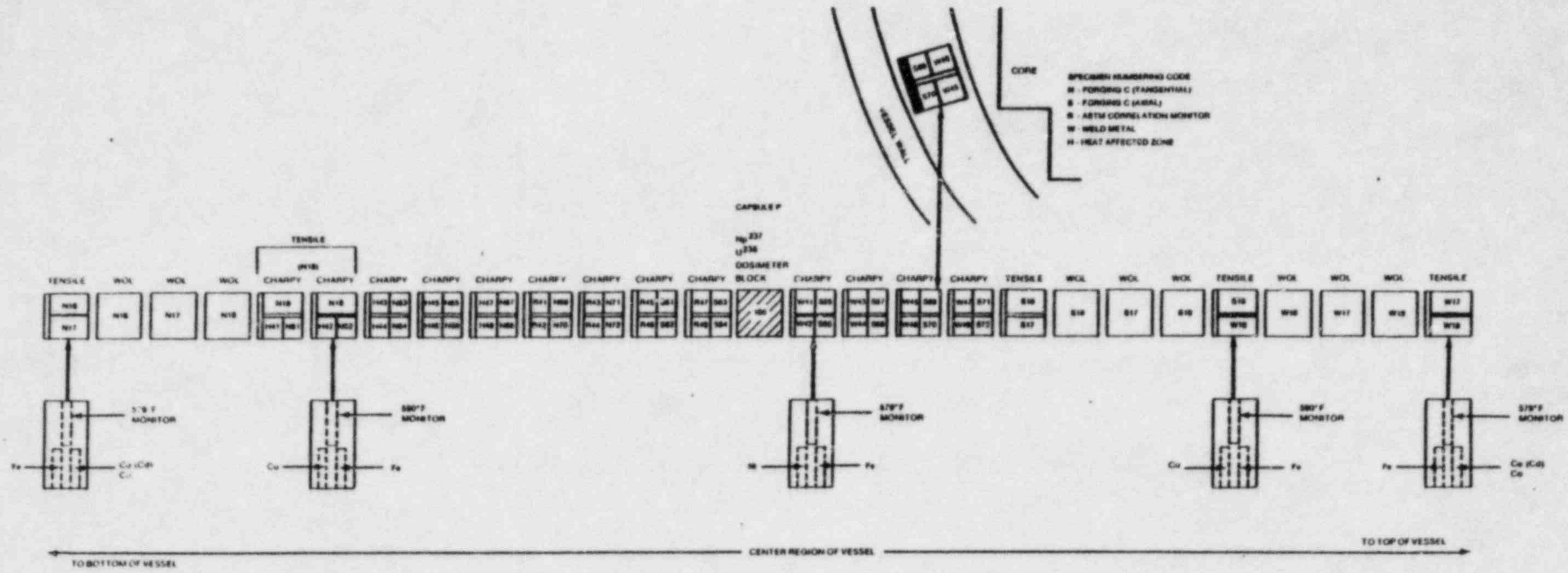

Figure 4-2. **Capsule P Schematic Showing Location of Specimens, Thermal Monitors, and Dosimeters**

SECTION 5
TESTING OF SPECIMENS FROM CAPSULE

5-1. OVERVIEW

The postirradiation mechanical testing of the Charpy V-notch and tensile specimens was performed at the Westinghouse Research and Development Hot Laboratory with consultation by Westinghouse Nuclear Energy Systems personnel.

Upon receipt of the capsule at the Laboratory, the specimens and spacer blocks were carefully removed, inspected for identification number, and checked against the master list in WCAP-8086.[1] No discrepancies were found.

A TMI Model TM 52004H impact test machine was used to perform tests on the irradiated Charpy V-notch specimens. Before initiating tests on the irradiated Charpy V specimens, the accuracy of the impact machine was checked with a set of standard specimens obtained from the Army Material and Mechanics Research Center in Watertown, Massachusetts. The results of the calibration testing showed that the machine was certified for Charpy V-notch impact testing.

The tensile tests were conducted on a screw-driven instron testing machine having a 20,000 pound capacity. A crosshead speed of 0.05 in./min was used. The deformation of the specimen was measured using a strain gage extensometer. The extensometer was calibrated before testing with a Sheffield high-magnification drum-type extensometer calibrator.

Elevated temperature tensile tests were conducted using a split-tube furnace. The specimens were held at temperature a minimum of 30 minutes to stabilize their temperature prior to testing. Temperature was monitored using a chromel-alumel thermocouple in contact with the upper and lower clevis-pin specimen grips. Temperature was controlled within plus or minus 5° F.

The load-extension data were recorded on the testing machine strip chart. The yield strength, ultimate tensile strength, and uniform elongation were determined from these charts. The reduction in area and total elongation were determined from specimen measurements.

5-2. CHARPY V-NOTCH IMPACT TEST RESULTS

Charpy V-notch impact test results for the reactor vessel beltline forging C material, weld metal and heat-affected zone (HAZ) material and ASTM correlation monitor material from HSST Plate 02 irradiated to a fluence of 1.25×10^{19} n/cm^2 are presented in Tables 5-1 through 5-3 and Figures 5-1 through 5-5, respectively. A summary of the increases in transition temperature and decrease in the upper shelf energy of the various surveillance materials is presented in Table 5-4 and shows that 30 and 50 ft lb transition temperature increases for the shell forging C and the weld metal and HAZ material are small (20 to 70° F) for a fluence of 1.25×10^{19} n/cm^2, therefore indicating that the materials are not very sensitive to radiation. A comparison of the transition temperature increases resulting from irradiation tests performed on the two Prairie Island Unit 1 capsules tested to date shown in Table 5-5 indicates the vessel materials are not very sensitive to radiation. Photographs of broken Charpy impact specimens from the surveillance forging, weld metal and heat-affected-zone are shown in Figures 5-6 through 5-10.

5-3. TENSILE TEST RESULTS

The results of tensile tests performed on specimens from shell forging C and the weld metal are shown in Table 5-6. A comparison of the unirradiated versus irradiated tensile properties is shown in Figures 5-11 through 5-13 for forging C and the weld metal. The small increases in yield strength of approximately 5 to 10 ksi resulting from irradiation to 1.25×10^{19} n/cm^2 tend to confirm that the reactor vessel beltline materials are not highly sensitive to radiation as also indicated by the Charpy V-notch tests. A typical load-displacement curve obtained for the tensile tests is shown in Figure 5-14. Photographs of broken tensile specimens from the surveillance forging and weld metal are shown in Figures 5-15 through 5-17.

5-4. WEDGE OPENING LOADING TESTS

The Wedge Opening Loading fracture mechanics specimens that were contained in Capsule P have been stored at the Westinghouse Research Laboratory on the recommendation of the United States Nuclear Regulatory Commission and will be tested at a later date. The results of these tests will be reported upon their completion.

TABLE 5-1

CHARPY V-NOTCH IMPACT DATA FOR THE PRAIRIE ISLAND UNIT 1
PRESSURE VESSEL SHELL FORGING C
IRRADIATED AT 550° F, FLUENCE 1.25 x 10^{19} n/cm^2 (E > 1 Mev)

Sample Number	Temperature		Impact Energy		Lateral Expansion		Shear (%)
	(°C)	(°F)	(J)	(ft lb)	(mm)	(mils)	
Tangential Orientation							
N-69	-46	-50	13.0	9.5	0.08	3.1	3
N-72	-32	-25	23.5	17.5	0.40	15.7	7
N-67	-23	-10	66.0	48.5	0.88	34.6	18
N-71	-18	0	59.5	44.0	0.91	35.8	17
N-61	-4	25	65.0	48.0	0.94	37.0	28
N-64	10	50	101.0	74.5	1.70	66.9	34
N-70	24	75	131.5	97.0	1.37	53.9	53
N-62	38	100	143.5	106.0	1.95	76.8	64
N-63	66	150	175.0	129.0	1.86	73.2	78
N-68	93	200	200.0	147.5	2.30	90.6	100
N-65	135	275	185.0	136.5	2.27	89.4	100
N-66	177	350	193.0	142.5	2.29	90.2	100
Axial Orientation							
S-71	-46	-50	8.0	6.0	0.31	12.2	3
S-66	-23	-10	25.0	18.5	0.40	15.7	13
S-72	-18	0	54.0	40.0	0.80	31.5	18
S-62	10	50	79.5	58.5	1.40	55.1	31
S-64	24	75	95.0	70.0	1.35	53.1	45
S-65	38	100	74.5	55.0	1.20	47.2	33
S-67	66	150	123.5	91.0	1.31	51.6	66
S-70	93	200	139.5	103.0	1.67	65.7	87
S-69	121	250	198.0	146.0	1.86	73.2	100
S-68	177	350	170.0	125.5	1.62	63.8	100
S-63	204	400	186.5	137.5	1.45	57.1	100

TABLE 5-2

CHARPY V-NOTCH IMPACT DATA FOR THE PRAIRIE ISLAND UNIT 1 PRESSURE VESSEL WELD AND HEAT-AFFECTED ZONE METAL IRRADIATED AT 550° F, FLUENCE 1.25 x 10^{19} n/cm² (E > 1 Mev)

Sample Number	Temperature		Impact Energy		Lateral Expansion		Shear
	(C°)	(°F)	(J)	(ft lb)	(mm)	(mils)	(%)
Weld Metal							
W-48	-46	-50	28.0	20.5	0.44	17.3	27
W-41	-32	-25	44.0	32.5	0.62	24.4	35
W-45	-18	0	48.0	35.5	0.71	28.0	43
W-44	10	50	70.0	51.5	0.94	37.0	53
W-46	24	75	75.0	55.5	1.32	52.0	71
W-42	66	150	96.5	71.0	1.69	66.5	95
W-47	121	250	129.0	95.0	1.96	77.2	100
W-43	149	300	113.0	83.5	1.97	77.6	100
HAZ Metal							
H-41	-101	-150	23.0	17.0	0.27	10.6	2
H-48	-73	-100	74.5	55.0	0.72	28.3	34
H-42	-18	0	111.0	82.0	1.16	45.7	79
H-43	24	75	252.0	186.0	1.68	66.1	96
H-47	66	150	158.0	116.5	1.76	69.3	96
H-46	121	250	173.0	127.5	2.04	80.3	100

TABLE 5-3

CHARPY V-NOTCH IMPACT DATA FOR THE PRAIRIE ISLAND UNIT 1
A533 GRADE B CLASS 1 CORRELATION MONITOR MATERIAL
IRRADIATED AT 550°F, FLUENCE 1.25 x 10^{19} n/cm^2 (E > 1 Mev)

Sample Number	Temperature		Impact Energy		Lateral Expansion		Shear
	(C°)	(°F)	(J)	(ft lb)	(mm)	(mils)	(%)
R-47	52	125	12.0	9.0	0.13	5.1	9
R-44	93	200	34.0	25.0	0.54	21.3	38
R-48	99	210	38.0	28.0	0.84	33.1	34
R-43	107	225	67.0	49.5	0.92	36.2	58
R-45	121	250	91.0	67.0	1.47	57.9	65
R-41	149	300	118.5	87.5	1.20	47.2	100
R-42	177	350	99.5	73.5	1.75	68.9	100
R-46	218	425	127.0	93.5	1.56	61.4	100

TABLE 5-4

THE EFFECT OF 550°F IRRADIATION AT 1.25 x 10^{19} n/cm^2 (E > 1 Mev) ON THE NOTCH TOUGHNESS PROPERTIES OF THE PRAIRIE ISLAND UNIT 1 REACTOR VESSEL IMPACT TEST SPECIMENS

	Average 50 ft lb Temp. (°F)			Average 35 mil Lateral Expansion Temp. (°F)			Average 30 ft lb Temp. (°F)			Average Energy Absorption at Full Shear (ft lb)		
Material	**Unirradiated**	**Irradiated**	**ΔT**	**Unirradiated**	**Irradiated**	**ΔT**	**Unirradiated**	**Irradiated**	**ΔT**	**Unirradiated**	**Irradiated**	**Δ(ft lb)**
Forging C (Axial)	4	55	51	-12	28	40	-27	10	37	143.0	136	7
Forging C (Tangential)	-5	20	25	-25	7	32	-25	-5	20	158.0	142	16
Weld Metal	-14	46	60	-45	25	70	-57	-15	42	78.5	83	4.5[a]
HAZ Metal	-170	-105	65	-175	-65	110	-200	-130	70	211.0	143	68
Correlation Monitor	81	232	151	53	218	165	49	205	156	123.5	85	38.5

a. Upper Shelf Energy Increase

TABLE 5-5

SUMMARY OF PRAIRIE ISLAND UNIT 1 REACTOR VESSEL SURVEILLANCE CAPSULE CHARPY IMPACT TEST RESULTS

Material	Fluence 10^{19} n/cm^2	50 ft lb Trans. Temp Increase (°F)	30 ft lb Trans. Temp Increase (°F)	Decrease In Upper Shelf Energy (ft lb)
Forging C (Axial)	0.546	15	24	12[a]
	1.25	51	37	7
Forging C (Tangential)	0.546	39	38	15
	1.25	25	20	16
Weld Metal	0.546	32	25	12.5[a]
	1.25	60	42	4.5[a]
HAZ Metal	0.546	0	0	—
	1.25	65	70	68
Correlation Monitor	0.546	113	110	32.5
	1.25	151	156	38.5

a. Upper Shelf Energy Increase

TABLE 5-6

IRRADIATED TENSILE PROPERTIES FOR THE PRAIRIE ISLAND UNIT 1 PRESSURE VESSEL SHELL FORGING C AND WELD METAL FLUENCE 1.25 x 10^{19} n/cm^2 (E > 1 Mev)

Material	Sample No.	Test Temp. (°F)	0.2% Yield Strength (ksi)	Ultimate Tensile Strength (ksi)	Fracture Load (kip)	Fracture Stress (ksi)	Fracture Strength (ksi)	Uniform Elongation (%)	Total Elongation (%)	Reduction in Area (%)
Forging C (Axial)	S-16	78	73.3	92.7	2.95	181.1	60.1	12.0	26.0	67
	S-18	200	70.3	88.1	2.65	177.2	54.0	10.4	23.7	70
	S-17	500	63.2	84.5	2.30	160.7	46.9	9.0	20.4	71
Forging C (Tangential)	N-16	78	73.3	92.7	2.70	180.5	55.0	11.3	25.8	70
	N-18	200	70.3	87.6	2.60	166.5	53.0	9.6	22.5	68
	N-17	500	64.2	84.5	2.60	195.9	53.0	9.8	20.5	73
Weld Metal	W-18	78	86.6	97.8	3.30	197.1	67.2	16.5	26.1	66
	W-17	200	80.5	91.7	3.15	190.8	64.2	12.5	25.5	66
	W-16	500	67.2	86.1	3.10	145.0	63.2	11.3	20.9	56

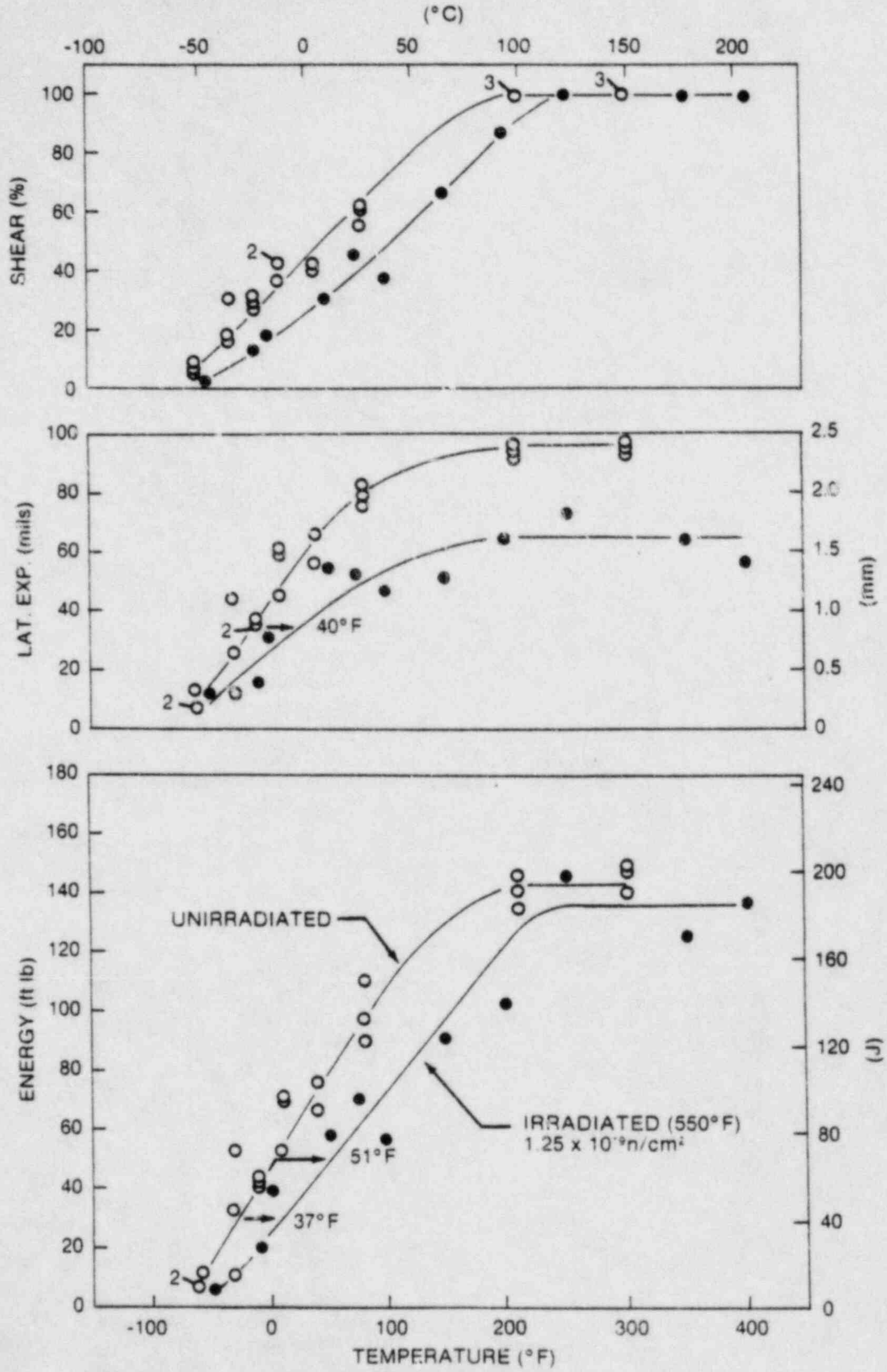

Figure 5-1. Irradiated Charpy V-Notch Properties for Prairie Island Unit 1 Reactor Vessel Shell Forging C (Axial Orientation)

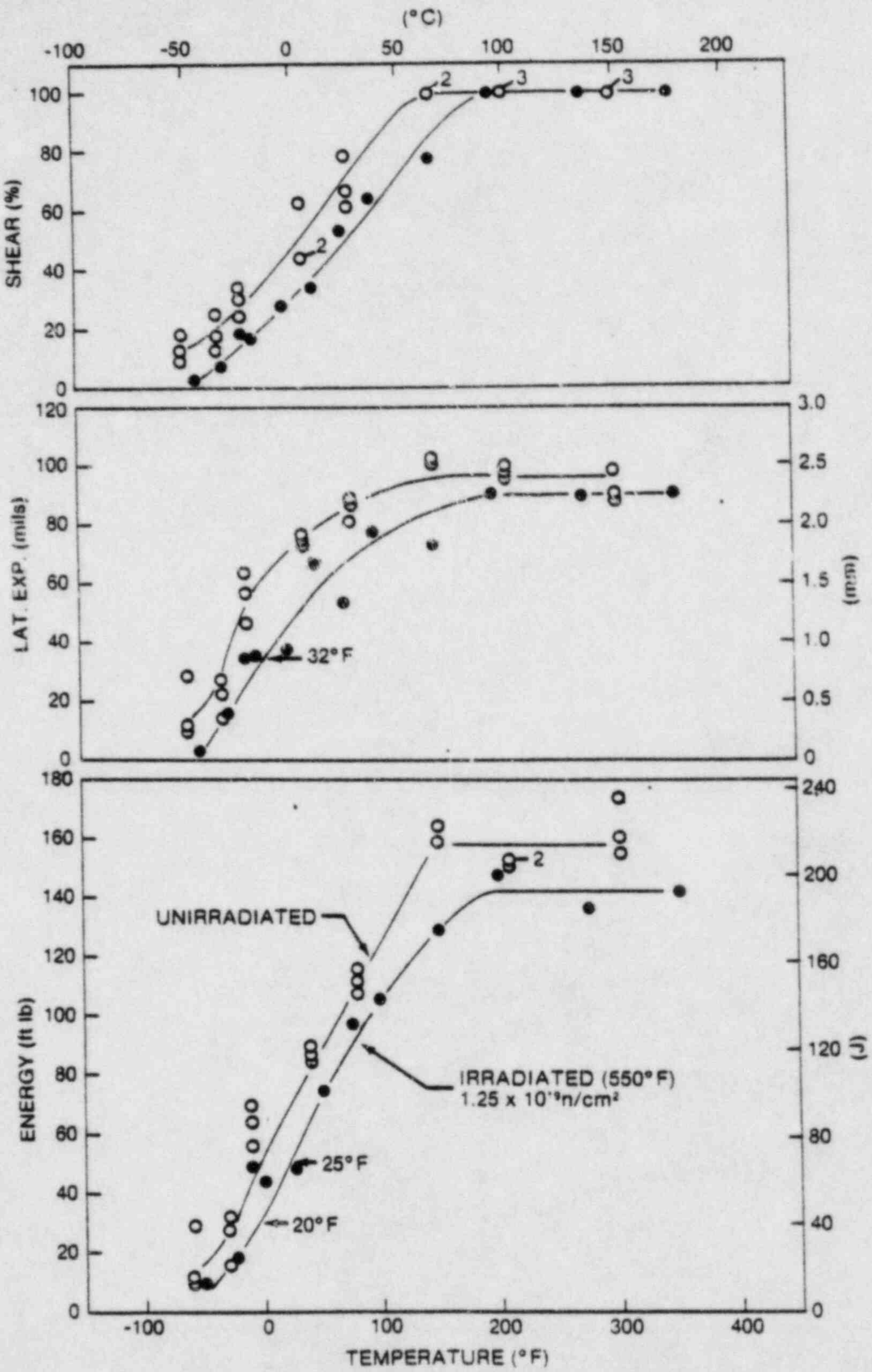

Figure 5-2. Irradiated Charpy V-Notch Properties for Prairie Island Unit 1 Reactor Vessel Shell Forging C (Tangential Orientation)

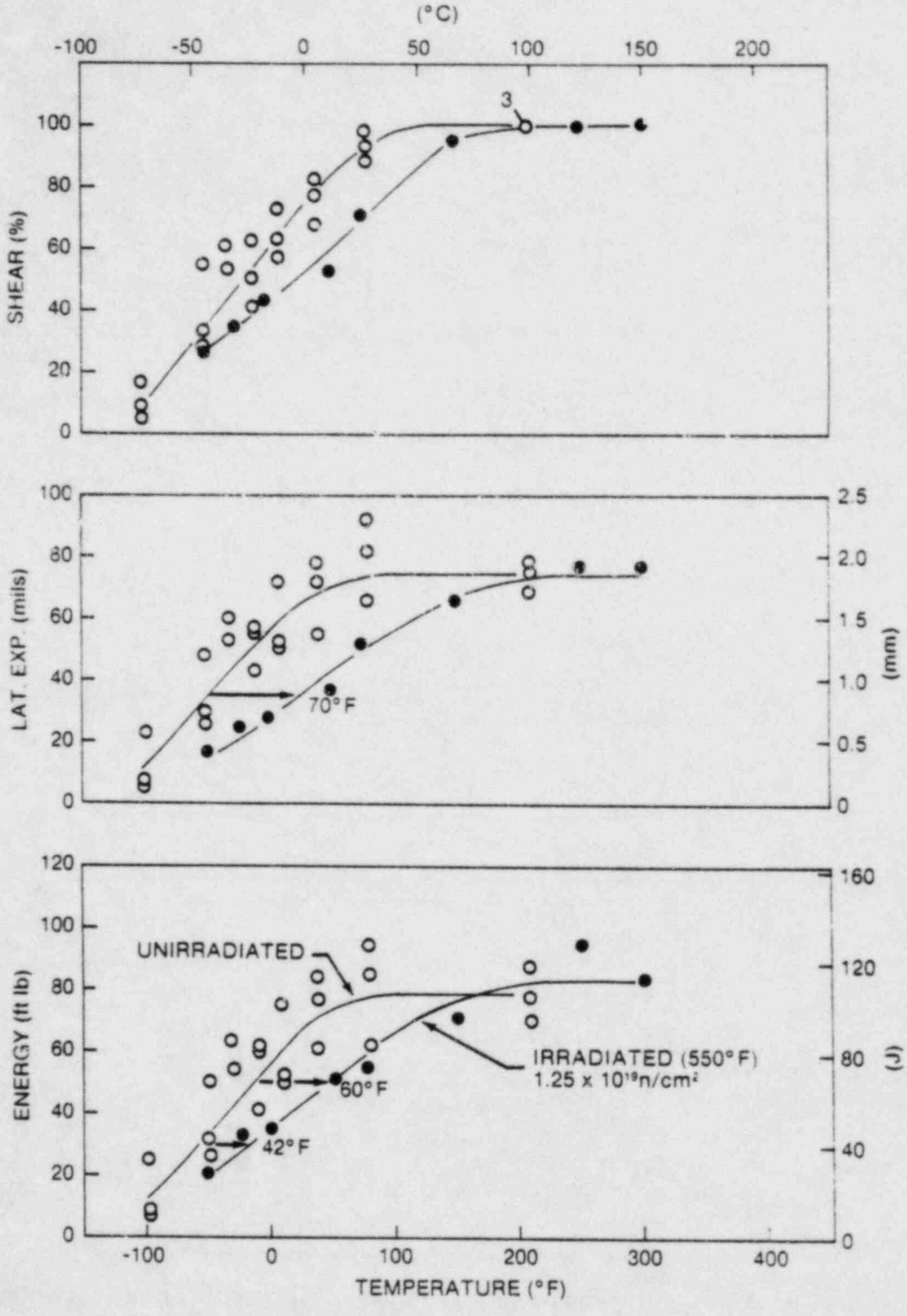

Figure 5-3. Irradiated Charpy V-Notch Properties for Prairie Island Unit 1 Reactor Pressure Vessel Weld Metal

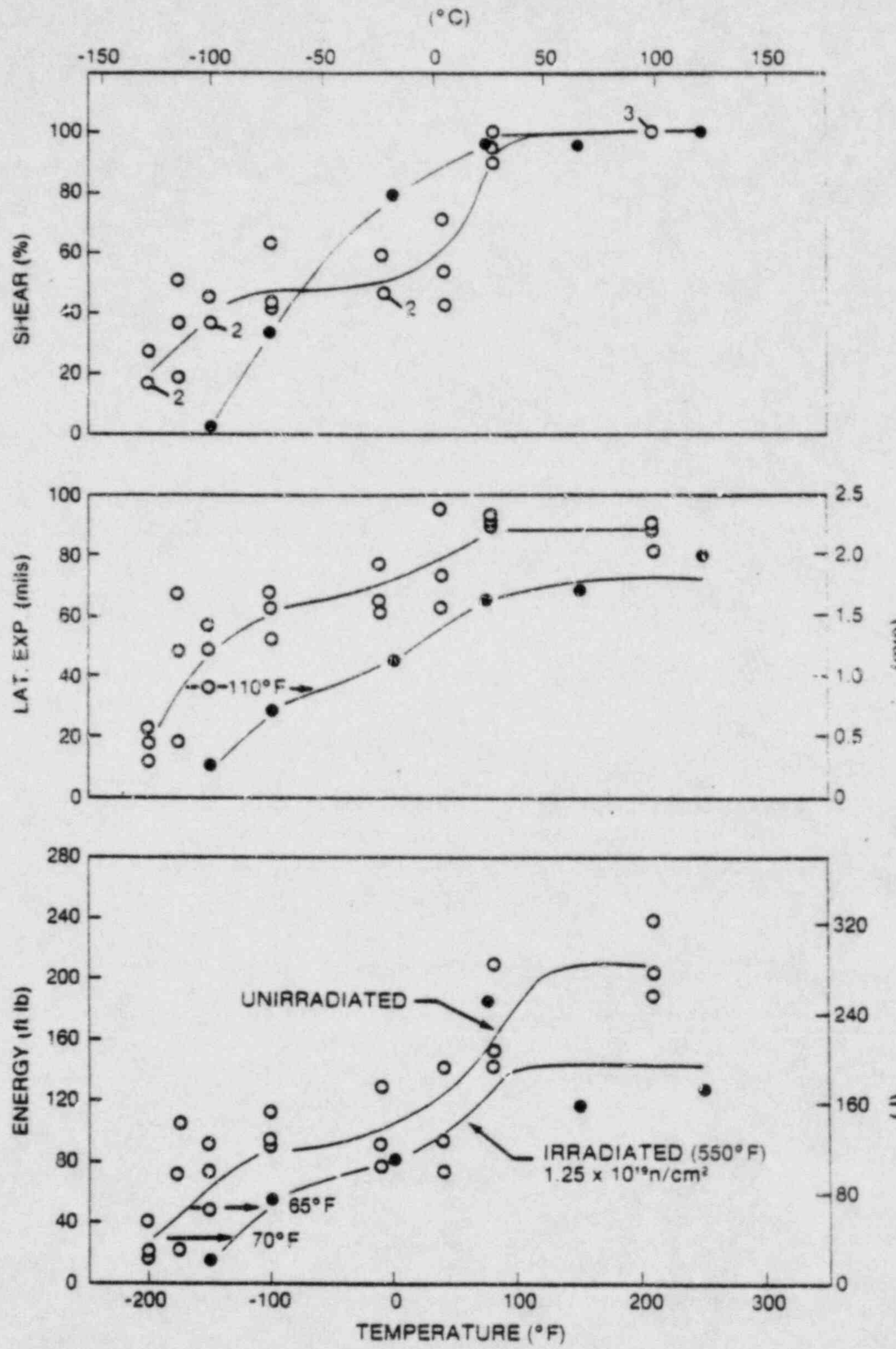

Figure 5-4. Irradiated Charpy V-Notch Properties for Prairie Island Unit 1 Reactor Pressure Vessel Weld Heat-Affected-Zone Metal

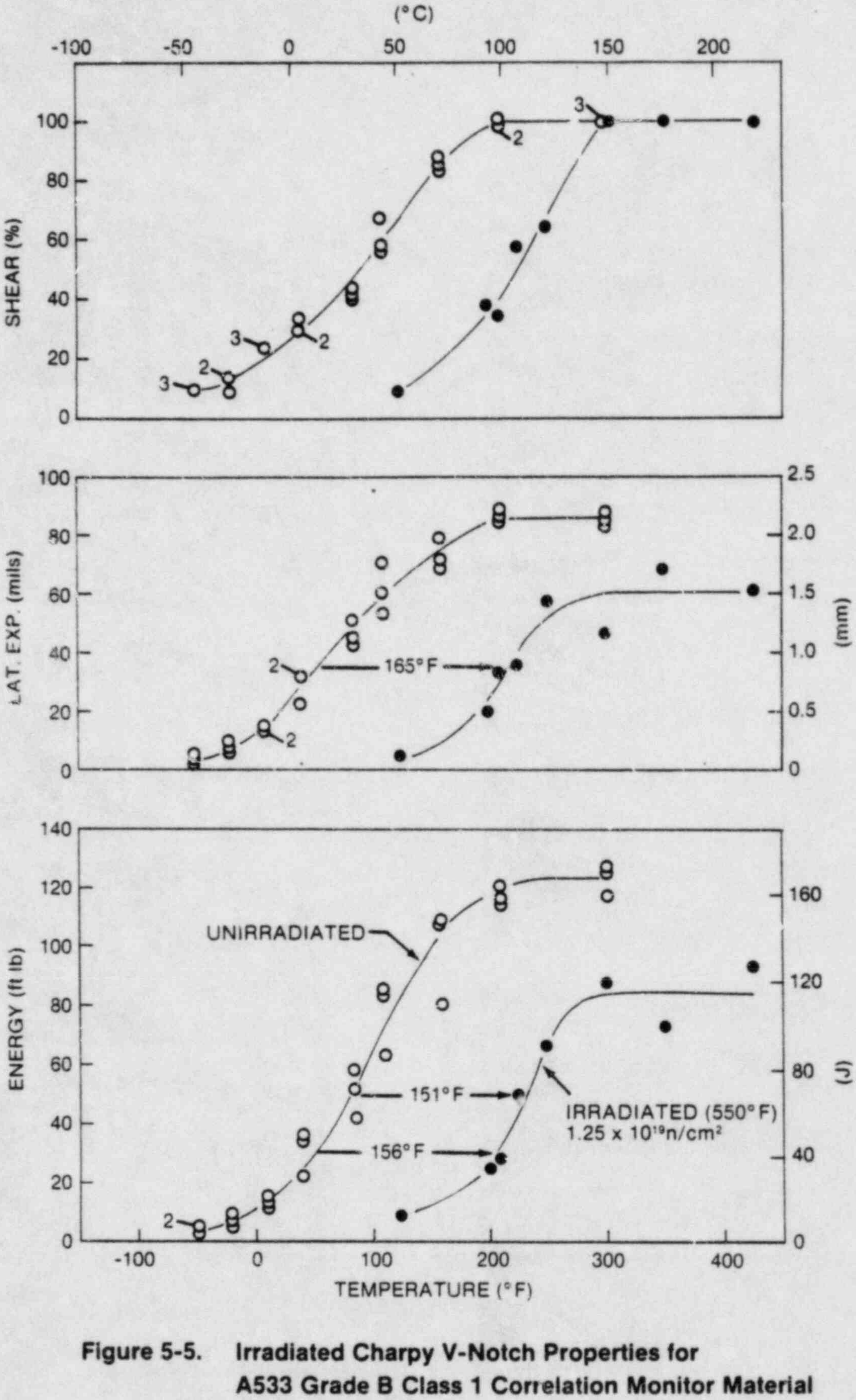

Figure 5-5. Irradiated Charpy V-Notch Properties for A533 Grade B Class 1 Correlation Monitor Material

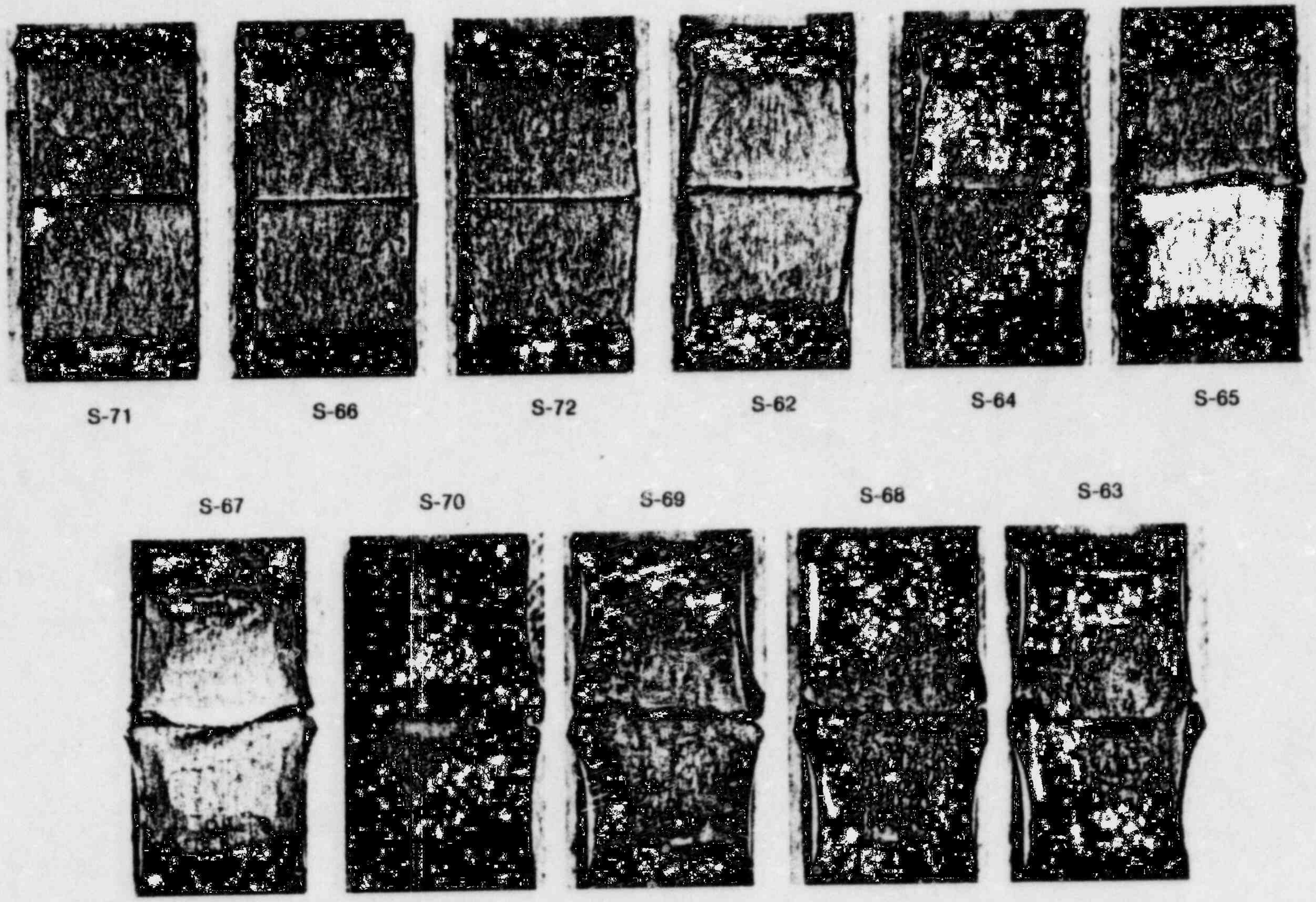

Figure 5-6. Charpy Impact Specimen Fracture Surfaces for Prairie Island Unit 1 Shell Forging C (Axial Orientation)

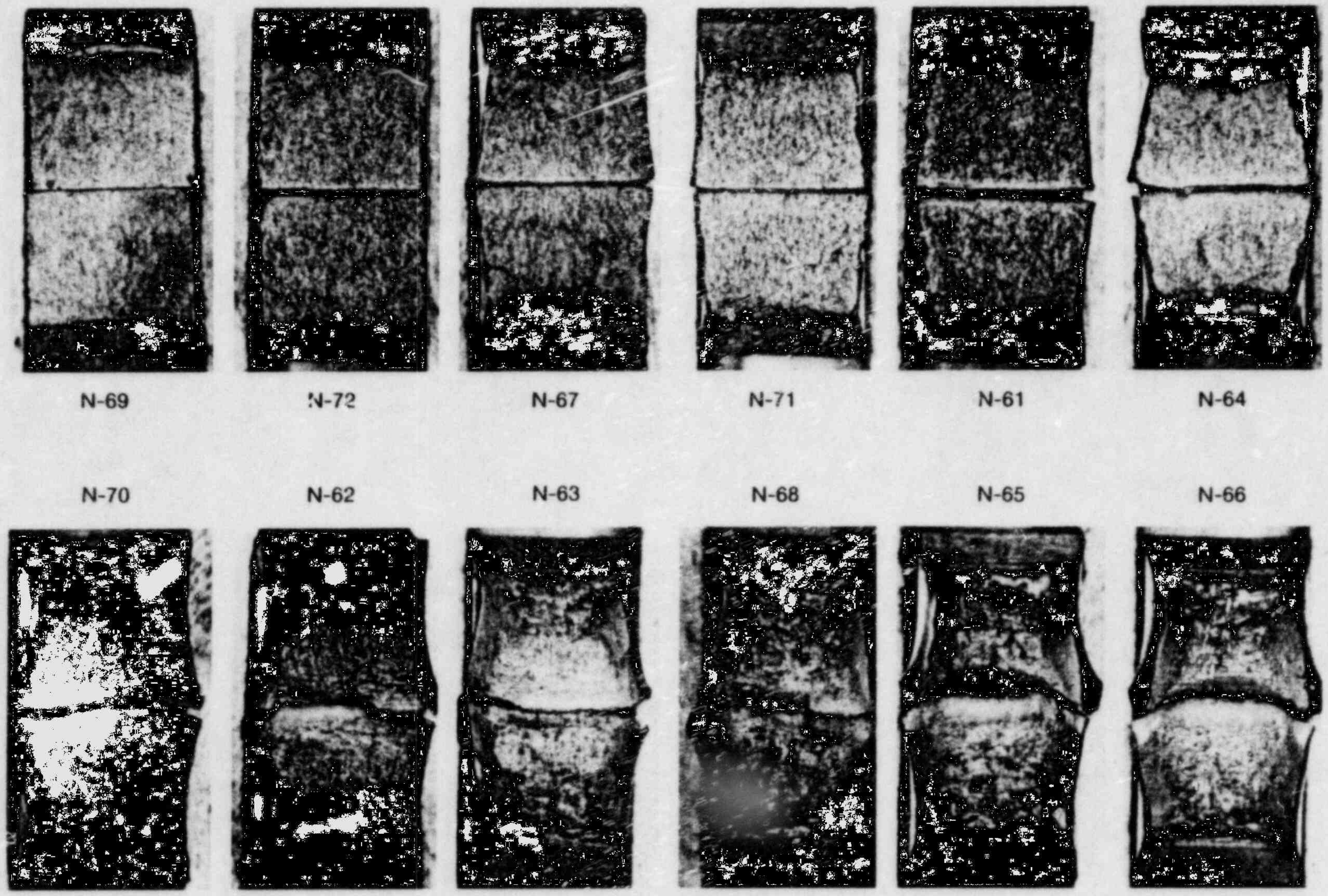

Figure 5-7. Charpy Impact Specimen Fracture Surfaces for Prairie Island Unit 1 Shell Forging C (Tangential Orientation)

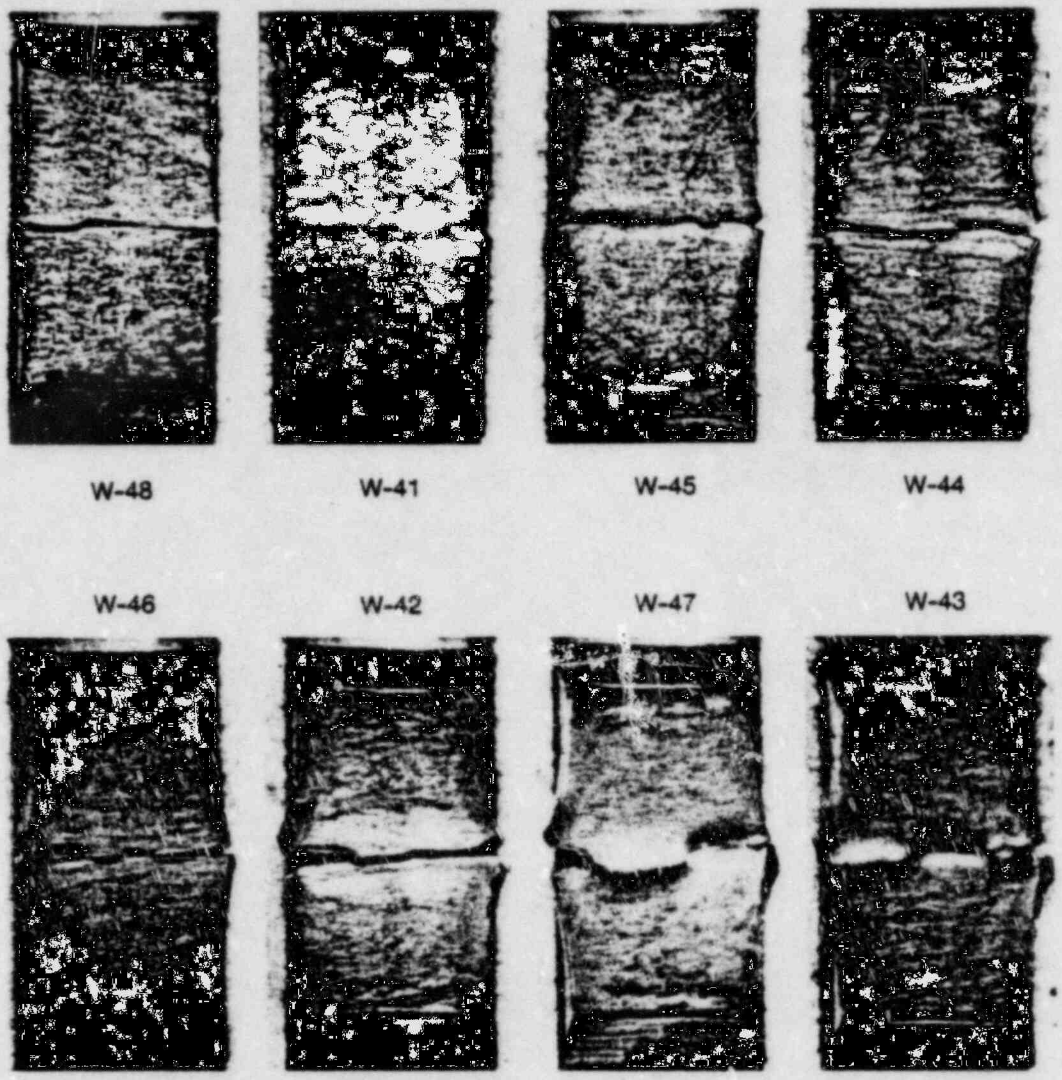

Figure 5-8. Charpy Impact Fracture Surfaces for Prairie Island Unit 1 Weld Metal

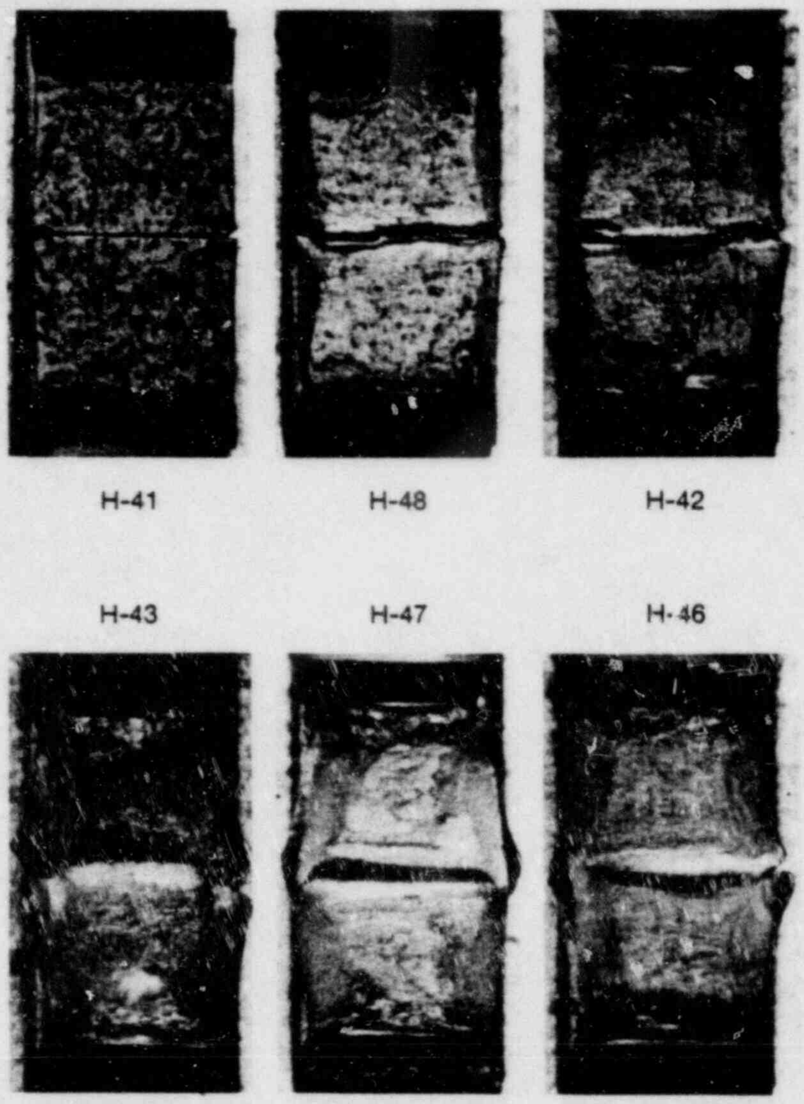

Figure 5-9. Charpy Impact Fracture Surfaces for Prairie Island Unit 1 Weld Heat-Affected-Zone Metal

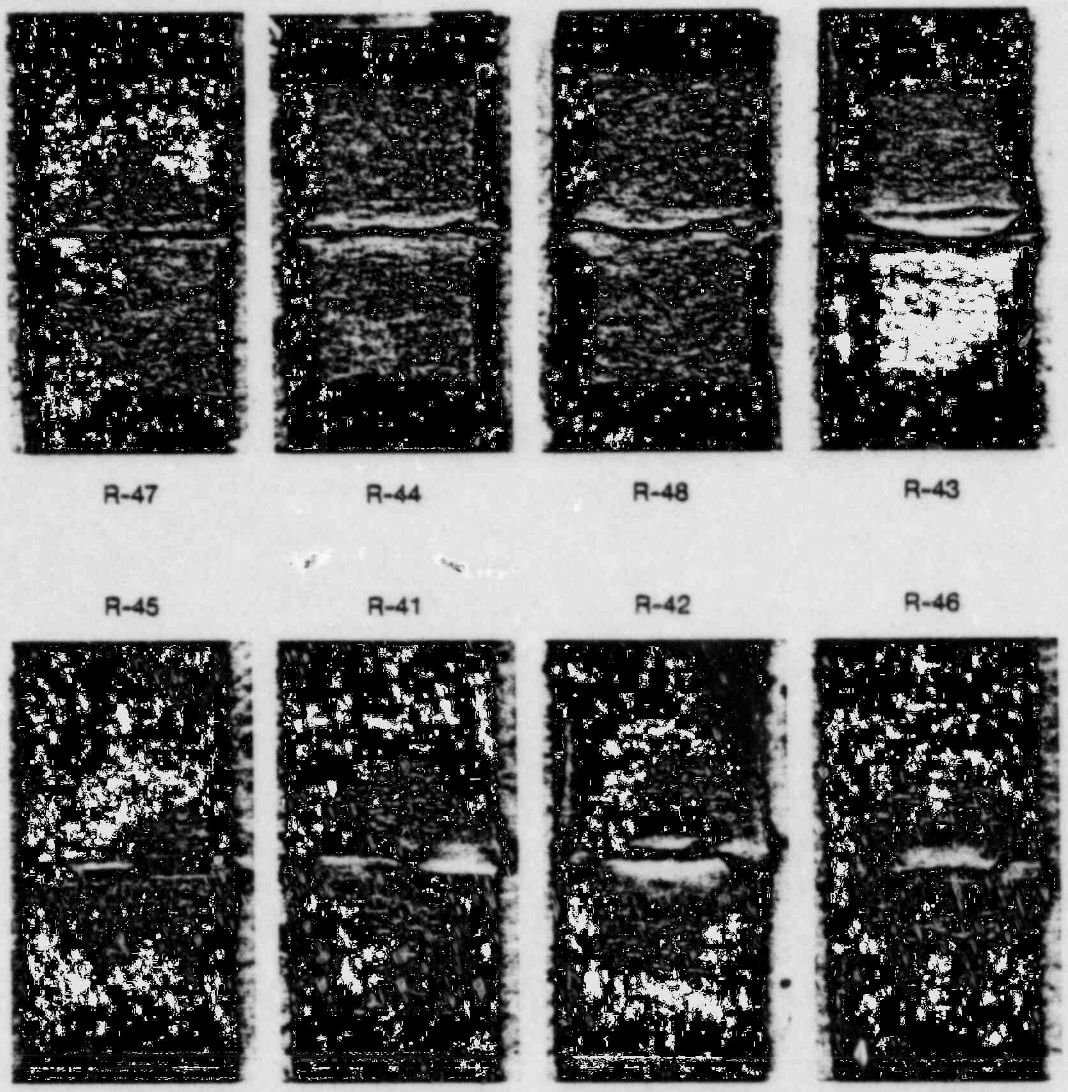

Figure 5-10. Charpy Impact Specimens Fracture Surfaces for Prairie Island Unit 1 A533 Grade B Class 1 Correlation Monitor Material

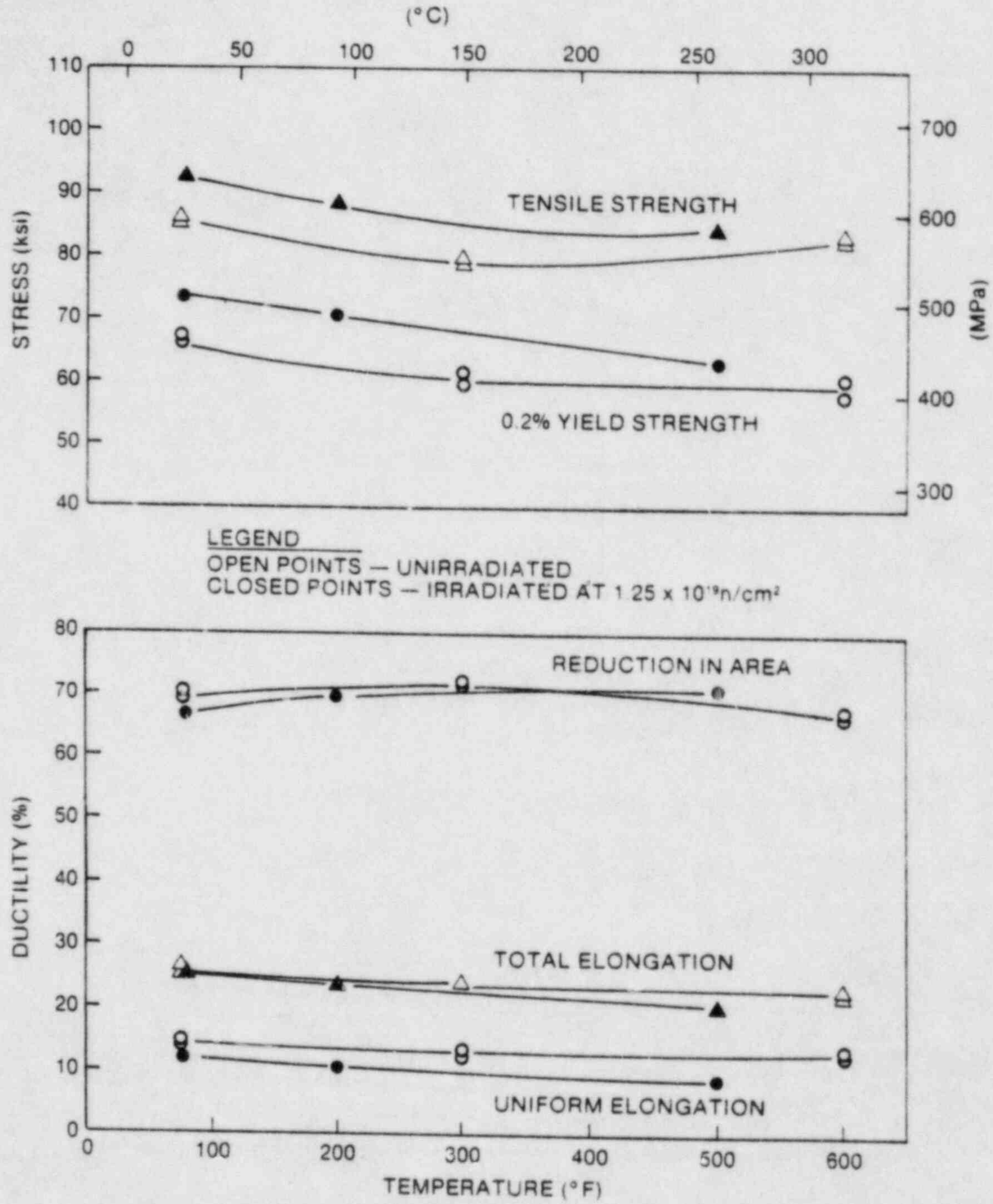

Figure 5-11. **Irradiated Tensile Properties for Prairie Island Unit 1 Reactor Pressure Vessel Shell Forging C (Axial Orientation)**

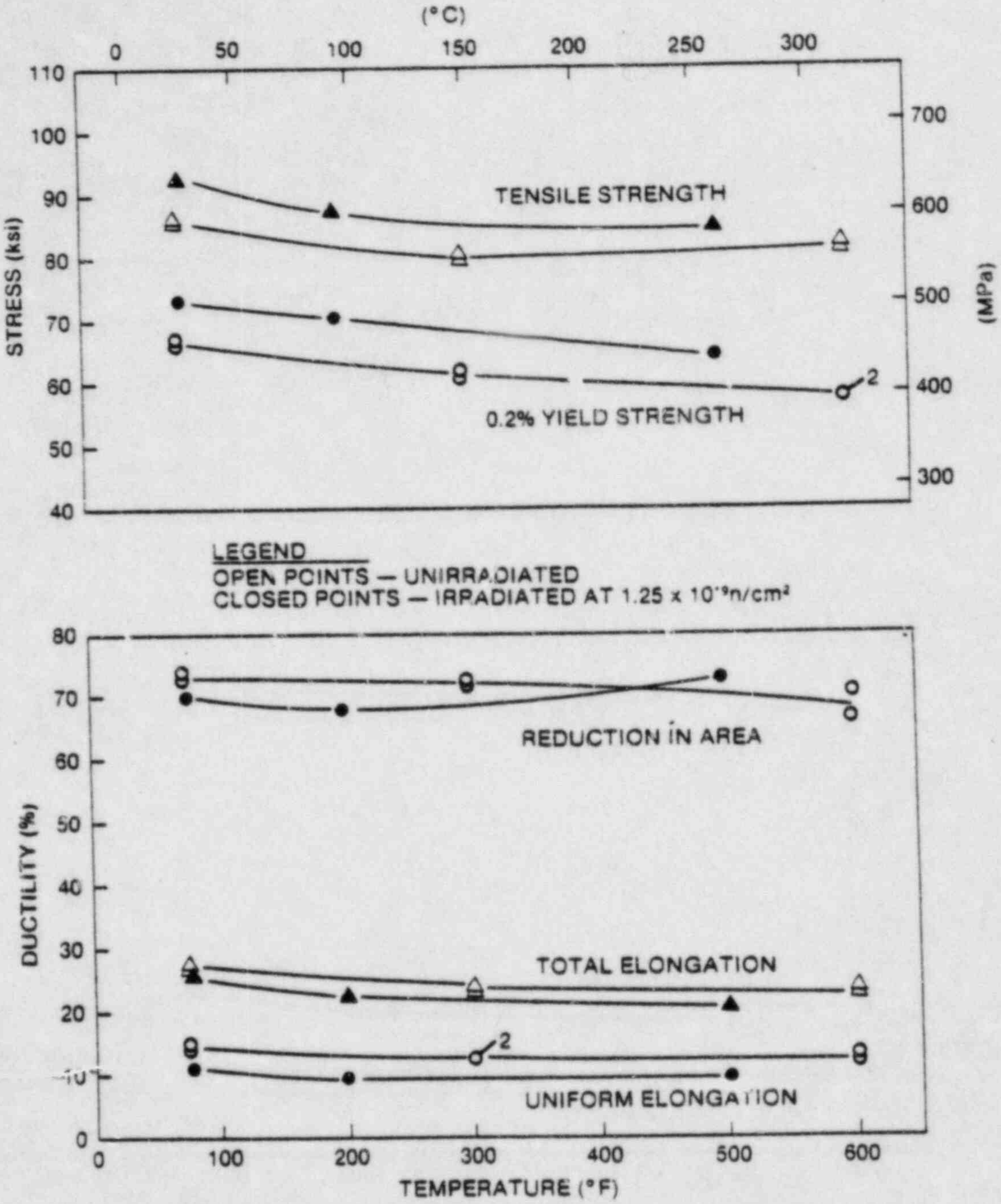

Figure 5-12. **Irradiated Tensile Properties for Prairie Island Unit 1 Reactor Pressure Vessel Shell Forging C (Tangential Orientation)**

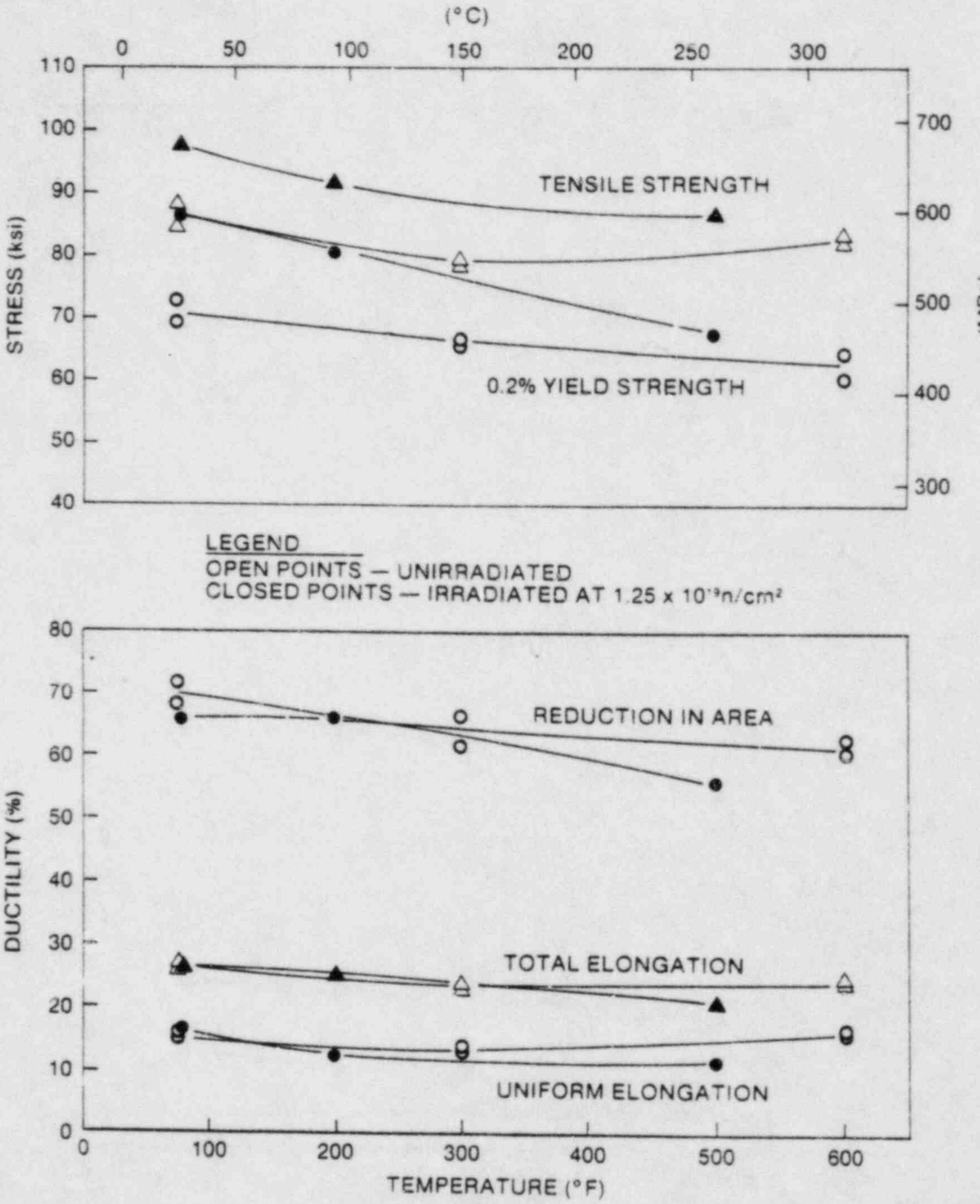

Figure 5-13. Irradiated Tensile Properties for Prairie Island Unit 1 Reactor Pressure Vessel Weld Metal

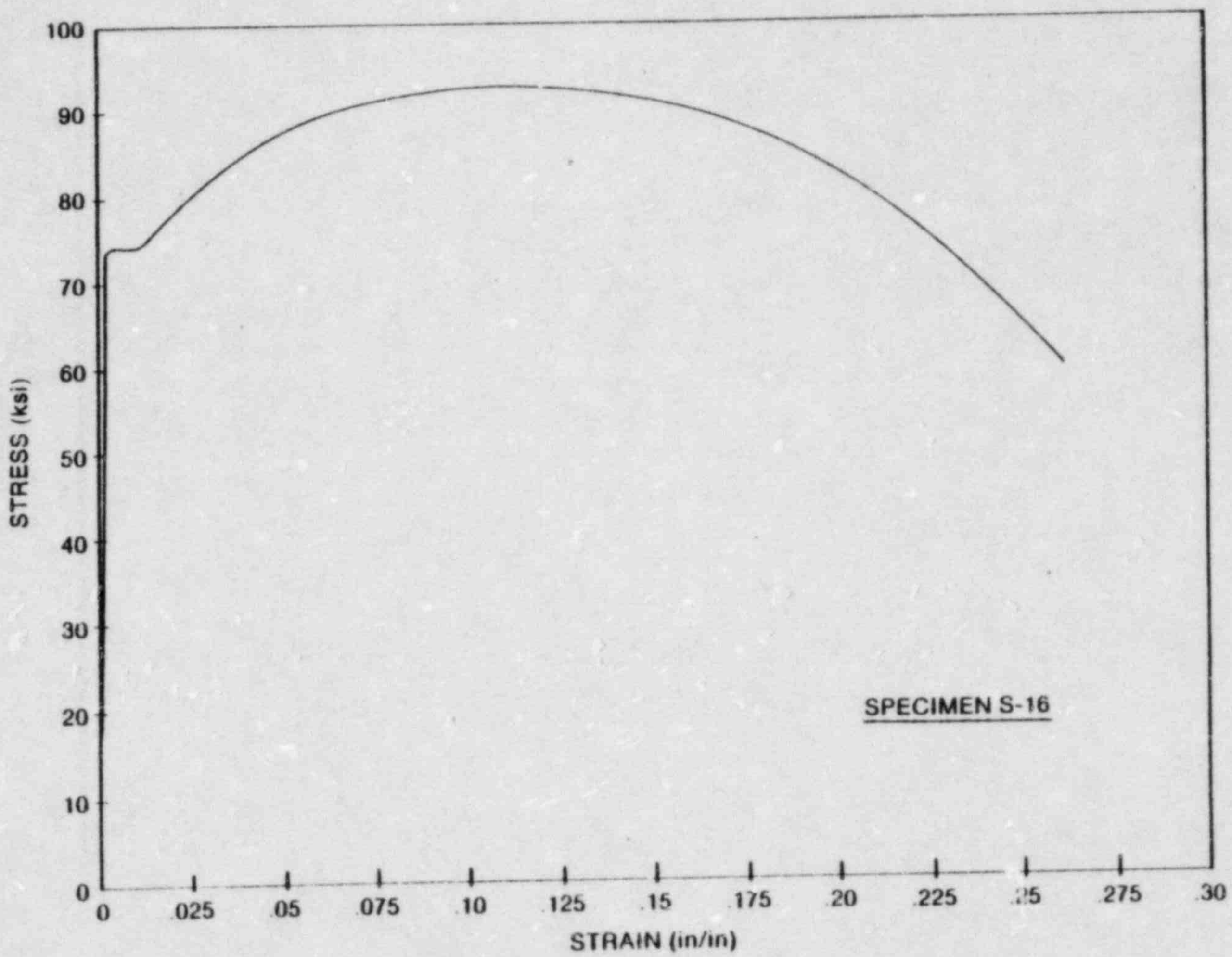

Figure 5-14. Typical Stress-Strain Curve for Tension Specimens

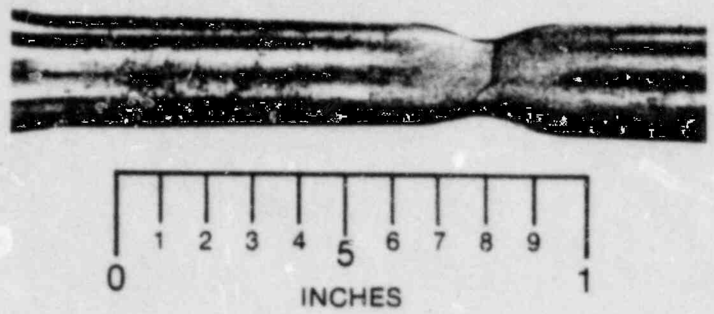

SPECIMEN S-16 78°F

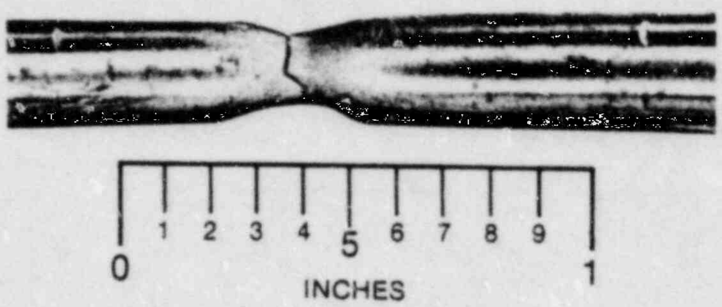

SPECIMEN S-18 200°F

SPECIMEN S-17 500°F

Figure 5-15. Fractured Tensile Specimens from Prairie Island Unit 1 Pressure Vessel Shell Forging C (Axial Orientation)

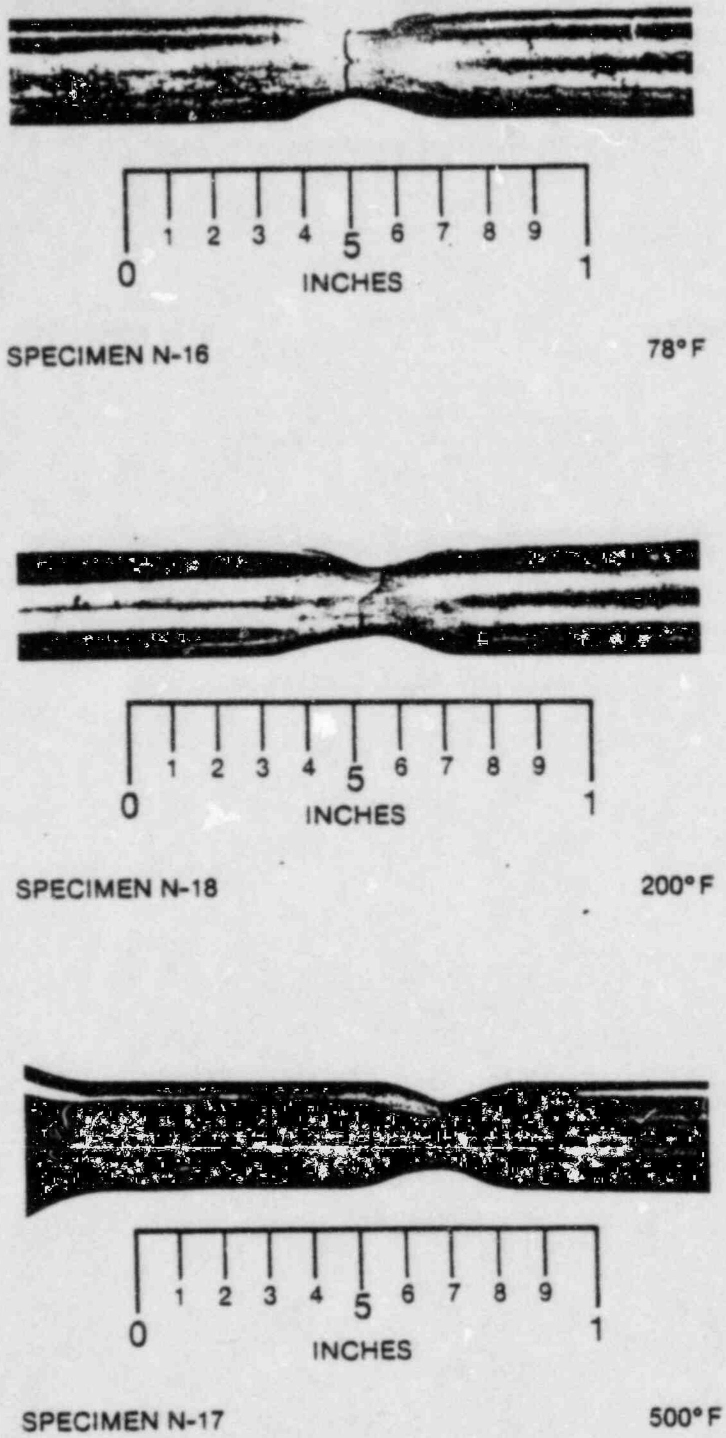

Figure 5-16. Fractured Tensile Specimens from Prairie Island Unit 1 Pressure Vessel Shell Forging C (Tangential Orientation)

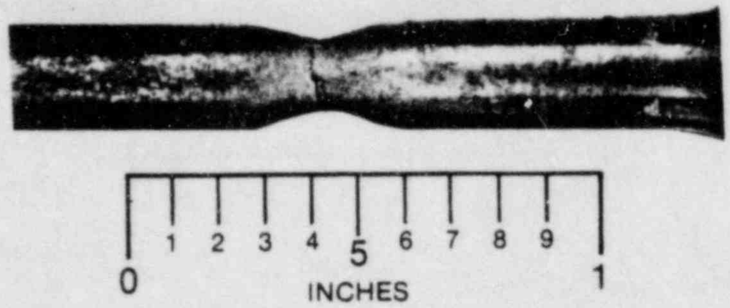

SPECIMEN W-18 78°F

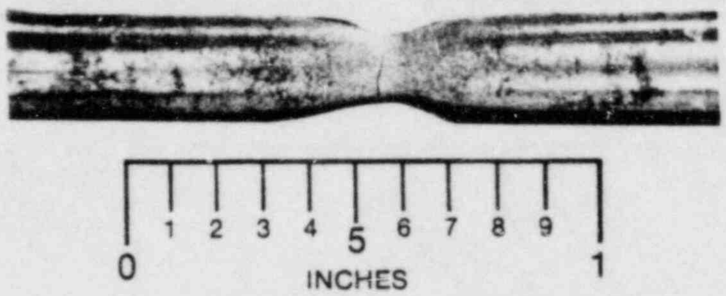

SPECIMEN W-17 200°F

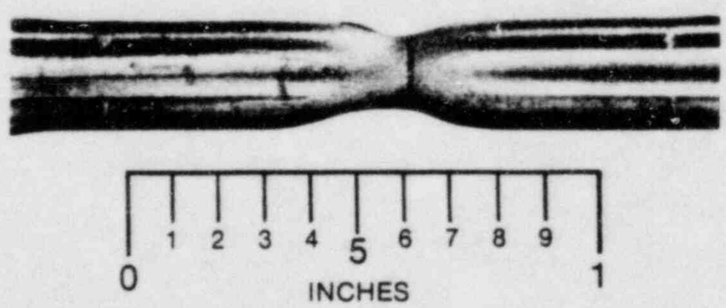

SPECIMEN W-16 500°F

Figure 5-17. Fractured Tensile Specimens from Prairie Island Unit 1 Pressure Vessel Weld Metal

SECTION 6
RADIATION ANALYSIS AND NEUTRON DOSIMETRY

6-1. INTRODUCTION

Knowledge of the neutron environment within the pressure vessel-surveillance capsule geometry is required as an integral part of LWR pressure vessel surveillance programs for two reasons. First, in the interpretation of radiation-induced property changes observed in materials test specimens, the neutron environment (fluence, flux) to which the test specimens were exposed must be known. Second, in relating the changes observed in the test specimens to the present and future condition of the reactor pressure vessel, a relationship between the environment at various positions within the reactor vessel and that experienced by the test specimens must be established. The former requirement is normally met by employing a combination of rigorous analytical techniques and measurements obtained with passive neutron flux monitors contained in each of the surveillance capsules. The latter information, on the other hand, is derived solely from analysis.

This section describes a discrete ordinates Sn transport analysis performed for the Prairie Island Unit 1 reactor to determine the fast neutron ($E > 1.0$ Mev) flux and fluence as well as the neutron energy spectra within the reactor vessel and surveillance capsules; and, in turn, to develop lead factors for use in relating neutron exposure of the pressure vessel to that of the surveillance capsules. Based on spectrum-averaged reaction cross sections derived from this calculation, the analysis of the neutron dosimetry contained in Capsule P is discussed and updated evaluations of dosimetry from Capsule V are presented.

6-2. DISCRETE ORDINATES ANALYSIS

A plan view of the Prairie Island reactor geometry at the core midplane is shown in Figure 6-1. Since the reactor exhibits 1/8th core symmetry, only a 0°-45° sector is depicted. Six irradiation capsules attached to the thermal shield are included in

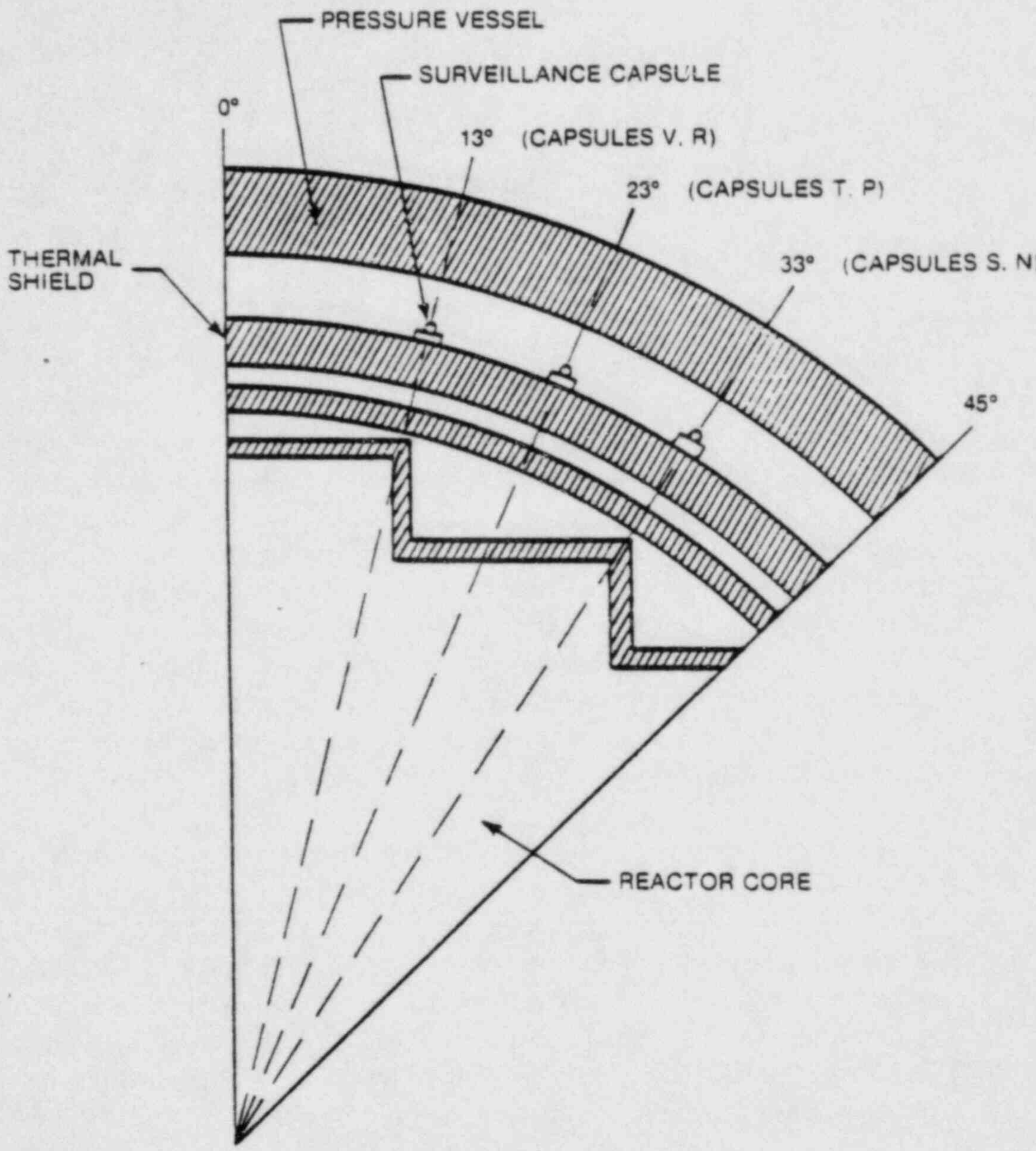

Figure 6-1. Prairie Island Unit 1 Reactor Geometry

the design to constitute the reactor vessel surveillance program. Two capsules are located symmetrically at 13°, 23° and 33° from the cardinal axis as shown in Figure 6-1.

A plan view of a single surveillance capsule attached to the thermal shield is shown in Figure 6-2. The stainless steel specimen container is 1-inch square and approximately 63 inches in height. The containers are positioned axially such that the specimens are centered on the core midplane, thus spanning the central 5.25 feet of the 12-foot-high reactor core.

From a neutronic standpoint, the surveillance capsule structures are significant. In fact, as will be shown later, they have a marked impact on the distributions of neutron flux and energy spectra in the water annulus between the thermal shield and the reactor vessel. Thus, in order to properly ascertain the neutron environment at the test specimen locations, the capsules themselves must be included in the analytical model. Use of at least a two-dimensional computation is, therefore, mandatory.

In the analysis of the neutron environment within the Prairie Island Unit 1 reactor geometry, predictions of neutron flux magnitude and energy spectra were made with the DOT[5] two-dimensional discrete ordinates code. The radial and azimuthal distributions were obtained from an R, Θ computation wherein the geometry shown in Figures 6-1 and 6-2 was described in the analytical model. In addition to the R, Θ computation, a second calculation in R, Z geometry was also carried out to obtain relative axial variations of neutron flux throughout the geometry of interest. In the R, Z analysis the reactor core was treated as an equivalent volume cylinder and, of course, the surveillance capsules were not included in the model.

Both the R, Θ and the R, Z analyses employed 21 neutron energy groups, an S_8 angular quadrature, and a P_1 cross-section expansion. The cross sections were generated via the Westinghouse GAMB1T[6] code system with broad group processing by the APPROPOS[7] and ANISN[8] codes. The energy group structure used in the analysis is listed in Table 6-1.

A key input parameter in the analysis of the integrated fast neutron exposure of the reactor vessel is the core power distribution. For the analysis, power distributions representative of time-averaged conditions derived from statistical studies of longterm operation of Westinghouse two-loop plants were employed. These input distributions include rod-by-rod spatial variations for all peripheral fuel assemblies.

It should be noted that this particular power distribution is intended to produce accurate end-of-life neutron exposure levels for the pressure vessel. As such, the calculation is indeed representative of an average neutron flux and small ($\pm$ 15-20%) deviations from cycle to cycle are to be expected.

TABLE 6-1.

21 GROUP ENERGY STRUCTURE

Group	Lower Energy (Mev)
1	7.79[a]
2	6.07
3	4.72
4	3.68
5	2.87
6	2.23
7	1.74
8	1.35
9	1.05
10	0.821
11	0.388
12	0.111
13	4.09×10^{-2}
14	1.50×10^{-2}
15	5.53×10^{-3}
16	5.83×10^{-4}
17	7.89×10^{-5}
18	1.07×10^{-5}
19	1.86×10^{-6}
20	3.00×10^{-7}
21	0.0

a. Upper energy of group 1 is 10.0 Mev.

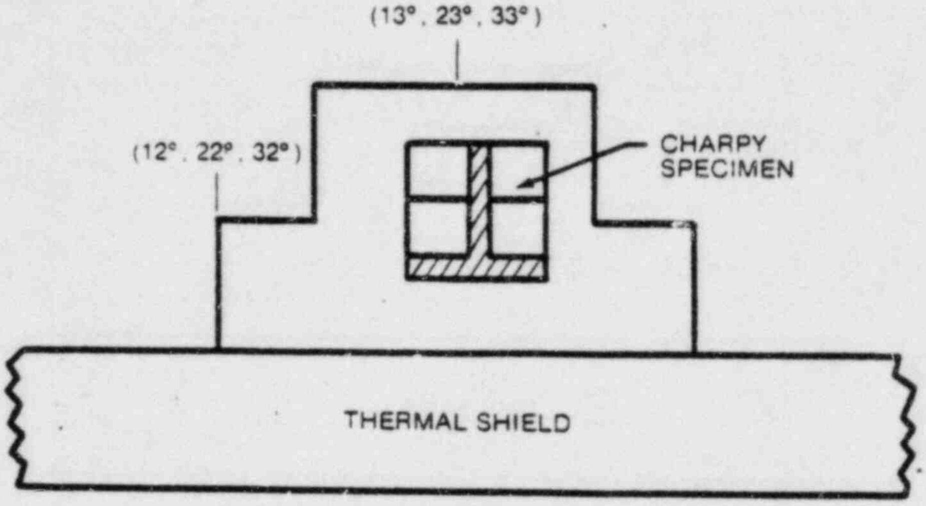

Figure 6-2. Plan View of a Reactor Vessel Surveillance Capsule

Having the results of the R,Θ and R,Z calculations, three-dimensional variations of neutron flux may be approximated by assuming that the following relation holds for the applicable regions of the reactor.

$$\phi(R,Z,\Theta,E_g) = \phi\ (R,Z,\Theta,E_g)\ F(Z,E_g) \qquad (6\text{-}1)$$

where:

$\phi(R,Z,\Theta,E_g)$ = neutron flux at point R,Z,Θ within energy group g

$\phi(R,\Theta,E_g)$ = neutron flux at point R,Θ within energy group g obtained from the R,Θ calculation

$F(Z,E_g)$ = relative axial distribution of neutron flux within energy group g obtained from the R,Z calculation

6-3. NEUTRON DOSIMETRY

The passive neutron flux monitors included in the Prairie Island Unit 1 surveillance program are listed in Table 6-2. The first five reactions in Table 6-2 are used as fast neutron monitors to relate neutron fluence ($E > 1.0$ Mev) to measured materials properties changes. To properly account for burnout of the product isotope generated by fast neutron reactions, it is necessary to also determine the magnitude of the thermal neutron flux at the monitor location. Therefore, bare and cadmium-covered cobalt-aluminum monitors were also included.

The relative locations of the various monitors within the surveillance capsules are shown in Figure 4-2. The nickel, copper, iron, and cobalt-aluminum monitors, in wire form, are placed in holes drilled in spacers at several axial levels within the capsules. The cadmium-shielded neptunium and uranium fission monitors are accommodated within the dosimeter block located near the center of the capsule.

The use of passive monitors such as those listed in Table 6-2 does not yield a direct measure of the energy-dependent flux level at the point of interest. Rather, the activation or fission process is a measure of the integrated effect that the time- and energy-dependent neutron flux has on the target material over the course of the irradiation period. An accurate assessment of the average neutron flux level incident on the various monitors may be derived from the activation measurements only if the irradiation parameters are well known. In particular, the following variables are of interest:

TABLE 6-2

NUCLEAR PARAMETERS FOR NEUTRON FLUX MONITORS

Monitor Material	Reaction of Interest	Target Weight Fraction	Response Range	Product Half-Life	Fission Yield (%)
Copper	$Cu^{63}(n,\alpha)Co^{60}$	0.6917	E>4.7 Mev	5.27 years	
Iron	$Fe^{54}(n,p)Mn^{54}$	0.0585	E>1.0 Mev	314 days	
Nickel	$Ni^{58}(n,p)Co^{58}$	0.6777	E>1.0 Mev	71.4 days	
Uranium-238[a]	$U^{238}(n,f)Cs^{137}$	1.0	E>0.4 Mev	30.2 years	6.3
Neptunium-237[a]	$Np^{237}(n,f)Cs^{137}$	1.0	E>0.08 Mev	30.2 years	6.5
Cobalt-Aluminum[a]	$Co^{59}(n,\gamma)Co^{60}$	0.0015	0.4eV<0.015 Mev	5.27 years	
Cobalt-Aluminum	$Co^{59}(n,\gamma)Co^{60}$	0.0015	E<0.0015 Mev	5.27 years	

a. Denotes that monitor is cadmium shielded.

- The operating history of the reactor
- The energy response of the monitor
- The neutron energy spectrum at the monitor location
- The physical characteristics of the monitor

The analysis of the passive monitors and subsequent derivation of the average neutron flux requires completion of two procedures. First, the disintegration rate of product isotope per unit mass of monitor must be determined. Second, in order to define a suitable spectrum averaged reaction cross section, the neutron energy spectrum at the monitor location must be calculated.

The specific activity of each of the monitors is determined using established ASTM procedures.[9,10,11,12,13] Following sample preparation, the activity of each monitor is determined by means of a lithium-drifted germanium, Ge(Li), gamma spectrometer. The overall standard deviation of the measured data is a function of the precision of sample weighing, the uncertainty in counting, and the acceptable error in detector calibration. For the samples removed from Prairie Island Unit 1, the overall 2σ deviation in the measured data is determined to be $\pm$ 10 percent. The neutron energy spectra are determined analytically using the method described in Section 6-1.

Having the measured activity of the monitors and the neutron energy spectra at the locations of interest, the calculation of the neutron flux proceeds as follows.

The reaction product activity in the monitor is expressed as

$$R = \frac{N_o}{A} f_i \, Y \int_E \sigma(E)\phi(E) \sum_{j=1}^{N} \frac{P_j}{P_{max}} \left(1 - e^{-\lambda t_j}\right) e^{-\lambda t_d} \qquad 6\text{-}2$$

where

R = induced product activity

N_o = Avagadro's number

A = atomic weight of the target isotope

f_i = weight fraction of the target isotope in the target material

Y = number of product atoms produced per reaction

$\sigma(E)$ = energy-dependent reaction cross section

$\phi(E)$ = energy-dependent neutron flux at the monitor location with the reactor at full power

P_j = average core power level during irradiation period j

P_{max} = maximum or reference core power level

λ = decay constant of the product isotope

t_j = length of irradiation period j

t_d = decay time following irradiation period j

Since neutron flux distributions are calculated using multigroup transport methods and, further, since the prime interest is in the fast neutron flux above 1.0 Mev, spectrum-averaged reaction cross sections are defined such that the integral term in equation (6-2) is replaced by the following relation.

$$\int_E \sigma(E)\ \phi(E)dE \ = \ \bar{\sigma}\,\phi(E > 1.0 \text{ Mev})$$

where:

$$\bar{\sigma} = \frac{\int_0^\infty \sigma(E)\,\phi\,(E)dE}{\int_{1.0\ Mev}^\infty \phi\,(E)dE} = \frac{\sum_{G=1}^{N} \sigma g\,\phi g}{\sum_{G=G_{1.0\ Mev}}^{N} \phi g}$$

Thus, equation (6-2) is rewritten

$$R = \frac{N_o}{A} f_i\,\gamma\,\sigma\,\phi\,(E > 1.0\ Mev) \sum_{j=1}^{N} \frac{P_j}{P_{max}} \,(1\text{-}e^{-\lambda t_j})\,e^{-\lambda t_d}$$

or, solving for the neutron flux,

$$\phi\,(E > 1.0\ Mev) = \frac{R}{\frac{N_o}{A} f_i\,\gamma\,\sigma \sum_{j=1}^{N} \frac{P_j}{P_{max}} \,(1\text{-}e^{-\lambda t_j})\,e^{-\lambda t_d}} \quad . \qquad \text{6-3}$$

The total fluence above 1.0 Mev is then given by

$$\Phi\,(E > 1.0\ Mev) = \phi\,(E > 1.0\ Mev) \sum_{j=1}^{N} \frac{P_j}{P_{max}}\, t_j \qquad \text{6-4}$$

where:

$$\sum_{j=1}^{N} \frac{P_j}{P_{max}} t_j = \text{total effective full power seconds of reactor operation up to the time of capsule removal}$$

An assessment of the thermal neutron flux levels within the surveillance capsules is obtained from the bare and cadmium-covered $Co^{59}(n,\delta)Co^{60}$ data by means of cadmium ratios and the use of a 37-barn 2200 m/sec cross section. Thus,

$$\phi_{Th} = \frac{R_{bare} \left\{ \frac{D-1}{D} \right\}}{\frac{N_o}{A} f_i \gamma \sigma \sum_{j=1}^{N} \frac{P_j}{P_{max}} (1-e^{-\lambda t_j}) e^{-\lambda t_d}} \qquad 6\text{-}5$$

where:

$$D \text{ is defined as } \frac{R_{bare}}{R_{Cd\ covered}}$$

6-4. TRANSPORT ANALYSIS RESULTS

Results of the S_n transport calculations for the Prairie Island Unit 1 reactor are summarized in Figures 6-3 through 6-8 and in Tables 6-3 through 6-5. In Figure 6-3, the calculated maximum neutron flux levels at the surveillance capsule centerline, pressure vessel inner radius, 1/4 thickness location, and 3/4 thickness location are presented as a function of azimuthal angle. The influence of the surveillance capsules on the fast neutron flux distribution is clearly evident. In Figure 6-4, the radial distribution of maximum fast neutron flux ($E > 1.0$ Mev) through the thickness of the reactor pressure vessel is shown. The relative axial variation of neutron flux within the vessel is given in Figure 6-5. Absolute axial variations of fast neutron flux may be obtained by multiplying the levels given in Figures 6-3 or 6-4 by the appropriate values from Figure 6-5.

In Figure 6-6 the radial variations of fast neutron flux within surveillance capsules V and P are presented. These data, in conjunction with the maximum vessel flux, are used to develop lead factors for each of the capsules. Here the lead factor is defined as the ratio of the fast neutron flux ($E > 1.0$ Mev) at the dosimeter block location (capsule center) to the maximum fast neutron flux at the pressure vessel inner radius. Updated lead factors for all of the Prairie Island Unit 1 surveillance capsules are listed in Table 6-3.

Since the neutron flux monitors contained with the surveillance capsules are not all located at the same radial location, the measured disintegration rates are analytically adjusted for the gradients that exist within the capsules so that flux and fluence levels may be derived on a common basis at a common location. This point of comparison was chosen to be the capsule center. Analytically determined reaction rate gradients for use in the adjustment procedures are shown in Figures 6-7 and 6-8 for Capsules V and P. All of the applicable fast neutron reactions are included.

In order to derive neutron flux and fluence levels from the measured disintegration rates, suitable spectrum-averaged reaction cross sections are required. The neutron energy spectrum calculated to exist at the center of each of the Prairie Island Unit 1 surveillance capsules is given in Table 6-4. The associated spectrum-averaged cross sections for each of the five fast neutron reactions are given in Table 6-5.

6-5. DOSIMETRY RESULTS

The irradiation history of the Prairie Island Unit 1 reactor is given in Table 6-6. Comparisons of measured and calculated saturated activity of the flux monitors contained in Capsules V and P are listed in Tables 6-7, and 6-8, respectively. The data are presented as measured at the actual monitor locations as well as adjusted to the capsule center. The measured results for both Capsules V and P were obtained by Westinghouse. All adjustments to the capsule centers were based on the data presented on Figures 6-7 and 6-8.

The fast neutron ($E > 1.0$ Mev) flux and fluence levels derived for Capsules V and P are presented in Table 6-9. The thermal neutron flux obtained from the cobalt-aluminum monitors is summarized in Table 6-10. Due to the relatively low thermal neutron flux at the capsule locations, no burnup correction was made to any of the measured activities. The maximum error introduced by this assumption is estimated to be less than 1 percent for the Ni^{58} (n,p) Co^{58} reaction and even less significant for all of the other fast neutron reactions.

Using the iron data presented in Table 6-9, along with the lead factors given in Table 6-3, the fast neutron fluence (E > 1.0 Mev) for Capsules V and P as well as for the reactor vessel inner diameter are summarized in Table 6-11 and Figure 6-9. The agreement between calculation and measurement is excellent, with measured fluence levels of 1.25×10^{19} and 5.46×10^{18} compared to calculated values of 1.21×10^{19} and 6.14×10^{18} n/cm² for Capsules P and V, respectively. Further, the graphical representation in Figure 6-9 indicates the accuracy of the transport analysis for Prairie Island Unit 1 and supports the use of the analytically determined fluence trend curve for predicting vessel toughness at times in the future. Projecting to end-of-life, a summary of peak fast neutron exposure of the Prairie Island Unit 1 reactor as derived from both calculation and measurement may be made as follows.

	Fast Neutron Fluence (n/cm²)		
	Surface	**1/4 T**	**3/4 T**
Capsule P	4.48×10^{19}	2.94×10^{19}	8.67×10^{18}
Capsule V	3.87×10^{19}	2.62×10^{19}	7.72×10^{18}
Average measurement	4.17×10^{19}	2.78×10^{19}	8.19×10^{18}
Calculation	4.30×10^{19}	2.87×10^{19}	8.46×10^{18}

These data are based on 32 full-power years of operation at 1650 MWt.

Based on the new capsule to vessel inner wall lead factors identified in Table 6-3 and the new capsule withdrawal schedule identified in ASTM E185-79, it is recommended that future capsules be removed from the reactor per the following schedule.

Capsule Identity	**Vessel Location**	**Lead Factor**	**Removal Time**	**Capsule Fluence (n/cm²)**
V	77°	3.37	1.34 EFPY[a]	5.46×10^{18}
P	247°	1.94	4.6 EFPY[a]	1.25×10^{19}
R	257°	3.37	6.0 EFPY	2.72×10^{19}
T	67°	1.94	15.0 EFPY	3.91×10^{19}
N	237°	1.79	32.0 EFPY	7.70×10^{19}
S	57°	1.79	Standby	———

a. These Capsules have been Removed.

TABLE 6-3

CALCULATED FAST NEUTRON FLUX (E > 1.0 MEV) AND LEAD FACTORS FOR PRAIRIE ISLAND UNIT 1 SURVEILLANCE CAPSULES

Capsule Identification	Azimuthal Location	ϕ (E>1.0 Mev) (n/cm^2-sec)	Lead Factor
V	13°	1.45×10^{11}	3.37
R	13°	1.45×10^{11}	3.37
T	23°	8.33×10^{10}	1.94
P	23°	8.33×10^{10}	1.94
S	33°	7.67×10^{10}	1.79
N	33°	7.67×10^{10}	1.79

TABLE 6-4

CALCULATED NEUTRON ENERGY SPECTRA AT THE DOSIMETER BLOCK LOCATION FOR PRAIRIE ISLAND UNIT 1 SURVEILLANCE CAPSULES

Group No.	Neutron Flux (n/cm^2-sec)		
	Capsules V & R	Capsules T & P	Capsules S & N
1	8.17×10^{8}	5.99×10^{8}	5.26×10^{8}
2	2.68×10^{9}	1.99×10^{9}	1.75×10^{9}
3	4.43×10^{9}	3.08×10^{9}	2.73×10^{9}
4	4.98×10^{9}	3.18×10^{9}	2.88×10^{9}
5	8.66×10^{9}	5.20×10^{9}	5.14×10^{9}
6	1.70×10^{10}	1.01×10^{10}	9.26×10^{9}
7	2.46×10^{10}	1.41×10^{10}	1.30×10^{10}
8	3.53×10^{10}	1.97×10^{10}	1.39×10^{10}
9	4.67×10^{10}	2.53×10^{10}	2.35×10^{10}
10	5.04×10^{10}	2.67×10^{10}	2.48×10^{10}
11	1.67×10^{11}	8.66×10^{10}	8.03×10^{10}
12	2.11×10^{11}	1.05×10^{11}	9.76×10^{10}
13	9.42×10^{10}	4.65×10^{10}	4.34×10^{10}
14	7.11×10^{10}	3.52×10^{10}	3.28×10^{10}
15	5.67×10^{10}	2.80×10^{10}	2.62×10^{10}
16	1.32×10^{11}	6.41×10^{10}	5.99×10^{10}
17	1.03×10^{11}	5.07×10^{10}	4.73×10^{10}
18	1.06×10^{11}	5.14×10^{10}	4.82×10^{10}
19	8.41×10^{10}	4.09×10^{10}	3.83×10^{10}
20	9.34×10^{10}	4.52×10^{10}	4.23×10^{10}
21	2.97×10^{11}	1.51×10^{11}	1.36×10^{11}

TABLE 6-5

SPECTRUM AVERAGED REACTION CROSS SECTIONS AT THE DOSIMETER BLOCK LOCATION FOR PRAIRIE ISLAND UNIT 1 SURVEILLANCE CAPSULES

Reaction	$\bar{\sigma}$ (barns)		
	Capsules V & R	Capsules T & P	Capsules S & N
$Fe^{54}(n,p)Mn^{54}$	0.0595	0.0683	0.0666
$Ni^{58}(n,p)Co^{58}$	0.0811	0.0912	0.0893
$Cu^{63}(n,\alpha)Co^{60}$	0.000404	0.000517	0.000494
$U^{238}(n,f)F.P.$	0.333	0.345	0.344
$Np^{237}(n,f)F.P.$	2.93	2.80	2.82

$$\bar{\sigma} = \frac{\int_{o}^{\infty} \sigma(E)\phi(E)dE}{\int_{1\ Mev}^{\infty} \phi(E)dE}$$

TABLE 6-6

IRRADIATION HISTORY OF PRAIRIE ISLAND UNIT 1 REACTOR VESSEL SURVEILLANCE CAPSULE P

Month	P_j (MW)	P_{max} (MW)	$\frac{P_j}{P_{max}}$	Irradiation Time (days)	Decay[a] Time (days)
12/73	107	1650	.065	31	2905
1/74	0	1650	.000	31	2874
2/74	480	1650	.291	28	2846
3/74	118	1650	.072	31	2815
4/74	480	1650	.291	30	2785
5/74	0	1650	.000	31	2754
6/74	0	1650	.000	30	2724
7/74	837	1650	.507	31	2693
8/74	1025	1650	.621	31	2662
9/74	163	1650	.099	30	2632
10/74	255	1650	.155	31	2601
11/74	1515	1650	.918	30	2571
12/74	1566	1650	.949	31	2540
1/75	1298	1650	.787	31	2509
2/75	1277	1650	.774	28	2481
3/75	1605	1650	.972	31	2450
4/75	1263	1650	.765	30	2420
5/75	903	1650	.547	31	2389
6/75	1286	1650	.779	30	2359
7/75	1231	1650	.746	31	2328
8/75	1044	1650	.633	31	2297
9/75	1097	1650	.665	30	2267
10/75	1370	1650	.830	31	2236
11/75	1534	1650	.930	30	2206
12/75	1545	1650	.936	31	2175
1/76	1534	1650	.930	31	2144
2/76	1140	1650	.691	29	2115

a. Decay times are referenced to December 14, 1981 and August 23, 1976 for monitors of Capsules P and V, respectively. The Np and U monitors of Capsule V were counted on August 25, 1976. Capsule V was removed in March, 1976.

TABLE 6-6 CONTINUED

IRRADIATION HISTORY OF PRAIRIE ISLAND UNIT 1 REACTOR VESSEL SURVEILLANCE CAPSULE P

Month	P_j (MW)	P_{max} (MW)	$\frac{P_j}{P_{max}}$	Irradiation Time (days)	Decay[a] Time (days)
3/76	114	1650	.069	31	2084
4/76	0	1650	.000	30	2054
5/76	940	1650	.570	31	2023
6/76	1490	1650	.903	30	1993
7/76	1442	1650	.874	31	1962
8/76	1523	1650	.923	31	1931
9/76	1033	1650	.626	30	1901
10/76	1612	1650	.977	31	1870
11/76	1580	1650	.958	30	1840
12/76	1589	1650	.963	31	1809
1/77	1566	1650	.949	31	1778
2/77	1501	1650	.910	28	1750
3/77	770	1650	.467	31	1719
4/77	0	1650	.000	30	1689
5/77	1338	1650	.811	31	1658
6/77	1462	1650	.886	30	1628
7/77	1551	1650	.940	31	1597
8/77	1559	1650	.945	31	1566
9/77	1523	1650	.923	30	1536
10/77	1509	1650	.914	31	1505
11/77	1573	1650	.953	30	1475
12/77	1609	1650	.975	31	1444
1/78	1561	1650	.946	31	1413
2/78	1508	1650	.914	28	1385
3/78	1238	1650	.751	31	1354
4/78	516	1650	.313	30	1324
5/78	1573	1650	.953	31	1293

a. Decay times are referenced to December 14, 1981 and August 23, 1976 for monitors of Capsules P and V, respectively. The Np and U monitors of Capsule V were counted on August 25, 1976. Capsule V was removed in March, 1976.

TABLE 6-6 CONTINUED

IRRADIATION HISTORY OF PRAIRIE ISLAND UNIT 1 REACTOR VESSEL SURVEILLANCE CAPSULE P

Month	P_j (MW)	P_{max} (MW)	$\frac{P_j}{P_{max}}$	Irradiation Time (days)	Decay[a] Time (days)
6/78	1496	1650	.907	30	1263
7/78	1156	1650	.700	31	1232
8/78	1349	1650	.818	31	1201
9/78	1353	1650	.820	30	1171
10/78	1577	1650	.956	31	1140
11/78	1485	1650	.900	30	1110
12/78	1582	1650	.959	31	1079
1/79	1588	1650	.963	31	1048
2/79	1600	1650	.970	28	1020
3/79	1516	1650	.919	31	989
4/79	247	1650	.150	30	959
5/79	982	1650	.595	31	928
6/79	1334	1650	.809	30	898
7/79	150	1650	.091	31	867
8/79	1263	1650	.766	31	836
9/79	1381	1650	.837	30	806
10/79	449	1650	.272	31	775
11/79	666	1650	.404	30	745
12/79	1462	1650	.886	31	714
1/80	1524	1650	.924	31	683
2/80	1206	1650	.731	29	654
3/80	1500	1650	.909	31	623
4/80	1482	1650	.898	30	593
5/80	1437	1650	.871	31	562
6/80	1395	1650	.845	30	532
7/80	474	1650	.288	31	501
8/80	1028	1650	.623	31	470

a. Decay times are referenced to December 14, 1981 and August 23, 1976 for monitors of Capsules P and V, respectively. The Np and U monitors of Capsule V were counted on August 25, 1976. Capsule V was removed in March, 1976.

TABLE 6-7

COMPARISON OF MEASURED AND CALCULATED FAST NEUTRON FLUX MONITOR SATURATED ACTIVITIES FOR CAPSULE P

Reaction and Axial Location	Radial Location (cm)	Saturated Activity (DPS/gm)		Adjusted Saturated Activity (DPS/gm)	
		Capsule P	Calculated	Capsule P	Calculated
$Fe^{54}(n,p)Mn^{54}$					
Top	157.87	4.25×10^6	3.83×10^6	4.10×10^6	
Mid-top	157.87	3.31×10^6	3.83×10^6	3.19×10^6	
Mid-bottom	157.87	3.93×10^6	3.83×10^6	3.80×10^6	
Bottom	157.87	4.41×10^6	3.83×10^6	4.25×10^6	
Average				3.84×10^6	3.70×10^6
$Cu^{63}(n,\alpha)Co^{60}$					
Mid-top	158.87	3.63×10^5	2.45×10^5	4.32×10^5	
Mid-bottom	158.87	3.38×10^5	2.45×10^5	4.01×10^5	
Average				4.17×10^5	2.91×10^5
$Ni^{58}(n,p)Co^{58}$					
Middle	158.87	5.41×10^7	4.51×10^6	6.45×10^7	5.38×10^7
$Np^{237}(n,f)Cs^{137}$					
Middle	158.10	4.48×10^7	3.69×10^7	4.48×10^7	3.69×10^7
$U^{238}(n,f)Cs^{137}$					
Middle	158.10	5.81×10^6	4.59×10^6	5.81×10^6	4.59×10^6

TABLE 6-8

COMPARISON OF MEASURED AND CALCULATED FAST NEUTRON FLUX MONITOR SATURATED ACTIVITIES FOR CAPSULE V

Reaction and Axial Location	Radial Location (cm)	Saturated Activity (DPS/gm)		Adjusted Saturated Activity (DPS/gm)	
		Capsule V	Calculated	Capsule V	Calculated
$Fe^{54}(n,p)Mn^{54}$					
Top	157.87	5.43×10^{6}	5.98×10^{6}	5.16×10^{6}	
Mid-top	157.87	4.99×10^{6}	5.98×10^{6}	4.74×10^{6}	
Middle	157.87	5.09×10^{6}	5.98×10^{6}	4.84×10^{6}	
Mid-bottom	157.87	5.28×10^{6}	5.98×10^{6}	5.02×10^{6}	
Bottom	157.87	5.64×10^{6}	5.98×10^{6}	5.36×10^{6}	
Average				5.02×10^{6}	5.68×10^{6}
$Cu^{63}(n,\alpha)Co^{60}$					
Mid-top	158.87	3.77×10^{5}	3.29×10^{5}	4.48×10^{5}	
Mid-bottom	158.87	4.26×10^{5}	3.29×10^{5}	5.07×10^{5}	
Average				4.77×10^{5}	3.91×10^{5}
$Ni^{58}(n,p)Co^{58}$					
Middle	158.87	6.29×10^{7}	7.17×10^{7}	7.44×10^{7}	8.48×10^{7}
$Np^{237}(n,f)Cs^{137}$					
Middle	158.10	6.11×10^{7}	7.01×10^{7}	6.11×10^{7}	7.01×10^{7}
$U^{238}(n,f)Cs^{137}$					
Middle	158.10	7.93×10^{6}	7.64×10^{6}	7.93×10^{6}	7.64×10^{6}

TABLE 6-9

RESULTS OF FAST NEUTRON DOSIMETRY FOR CAPSULES P AND V

		Adjusted Saturated Activity (DPS/gm)		$\phi(E > 1.0$ Mev) (n/cm^2-sec)		$\phi(E > 1.0$ Mev) (n/cm^2)	
Capsule	**Reaction**	**Measured**	**Calculated**	**Measured**	**Calculated**	**Measured**	**Calculated**
P	$Fe^{54}(n,p)Mn^{54}$	3.84×10^{6}	3.70×10^{6}	8.61×10^{10}	8.33×10^{10}	1.25×10^{19}	1.21×10^{19}
	$Cu^{63}(n,\alpha)Co^{60}$	4.17×10^{5}	2.91×10^{5}	1.22×10^{11}		1.77×10^{19}	
	$Ni^{58}(n,p)Co^{58}$	6.45×10^{7}	5.38×10^{7}	1.01×10^{11}		1.46×10^{19}	
	$Np^{237}(n,f)Cs^{137}$	4.48×10^{7}	3.69×10^{7}	9.68×10^{10}		1.40×10^{19}	
	$U^{238}(n,f)Cs^{137}$	5.81×10^{6}	4.59×10^{6}	1.06×10^{11}		1.53×10^{19}	
V	$Fe^{54}(n,p)Mn^{54}$	5.02×10^{6}	5.68×10^{6}	1.29×10^{11}	1.45×10^{11}	5.46×10^{18}	6.14×10^{18}
	$Cu^{63}(n,\alpha)Co^{60}$	4.77×10^{5}	3.91×10^{5}	1.79×10^{11}		7.58×10^{18}	
	$Ni^{58}(n,p)Co^{58}$	7.44×10^{7}	8.48×10^{7}	1.30×10^{11}		5.50×10^{18}	
	$Np^{237}(n,f)Cs^{137}$	6.11×10^{7}	7.01×10^{7}	1.37×10^{11}		5.80×10^{18}	
	$U^{238}(n,f)Cs^{137}$	7.93×10^{6}	7.64×10^{6}	1.50×10^{11}		6.35×10^{18}	

TABLE 6-10

RESULTS OF THERMAL NEUTRON DOSIMETRY FOR CAPSULES P AND V

Capsule	Axial Location	Saturated Activity (dps/gm)		ϕTh (n/cm^2-sec)
		Bare	Cd-covered	
P	Top	7.56×10^7	2.67×10^7	8.58×10^{10}
	Bottom	9.02×10^7	2.84×10^7	1.09×10^{11}
V	Top	1.90×10^7	8.25×10^6	1.28×10^{11}
	Bottom	2.23×10^7	7.68×10^6	1.73×10^{11}

TABLE 6-11

SUMMARY OF NEUTRON DOSIMETRY RESULTS FOR CAPSULES P AND V

Capsule	Irradiation Time (EFPS)	$\phi(E > 1.0$ Mev) (n/cm^2-sec)	$\phi(E > 1.0$ Mev) (n/cm^2)	Lead Factor	Vessel Fluence (n/cm^2)	Calculated Vessel Fluence (n/cm^2)
P	1.45×10^8	8.61×10^{10}	1.25×10^{19}	1.94	6.44×10^{18}	6.23×10^{18}
V	4.23×10^7	1.29×10^{11}	5.46×10^{18}	3.37	1.62×10^{18}	1.82×10^{18}

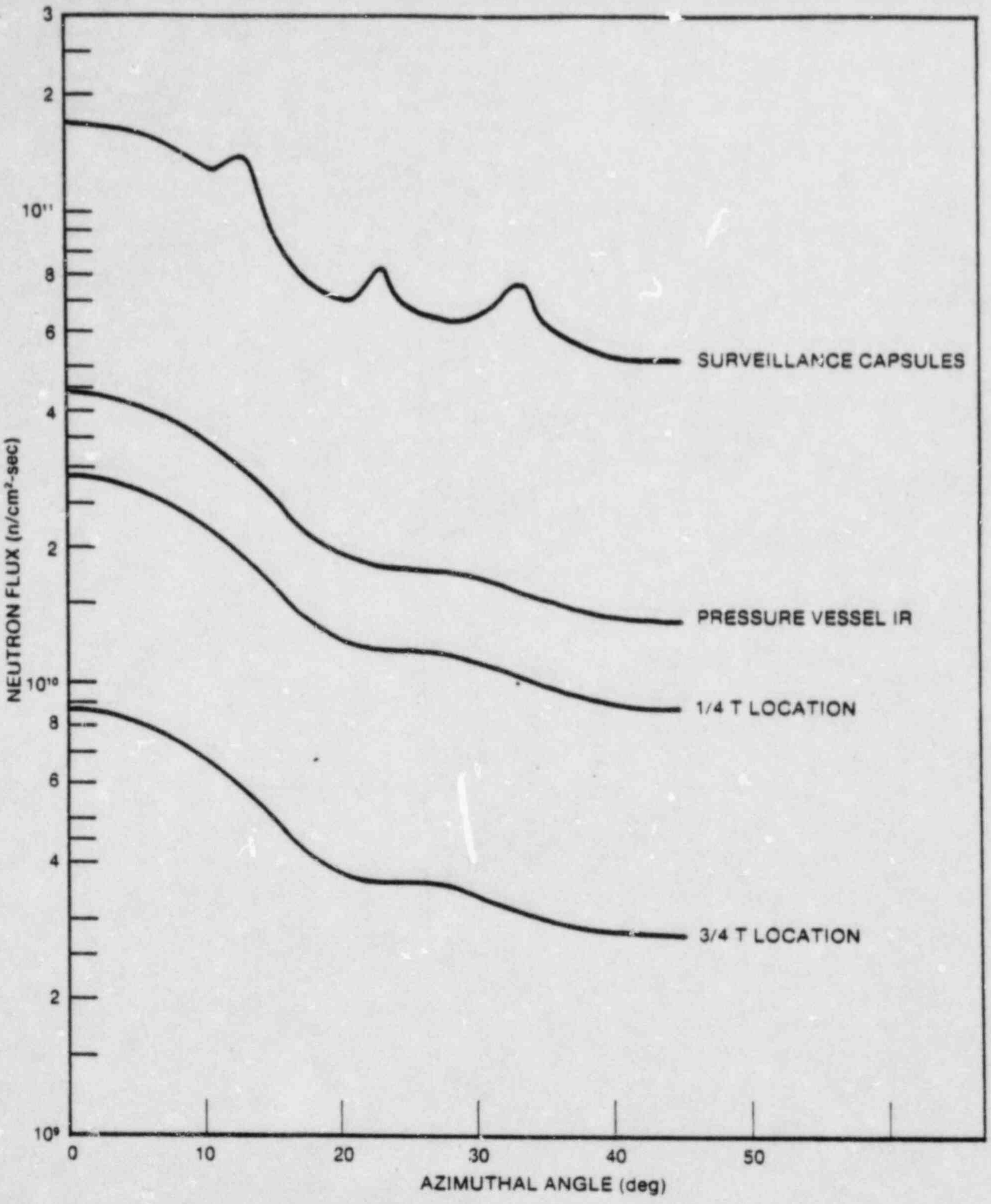

Figure 6-3. Calculated Azimuthal Distribution of Maximum Fast Neutron Flux (E > 1.0 Mev) within the Pressure Vessel Surveillance Capsule Geometry

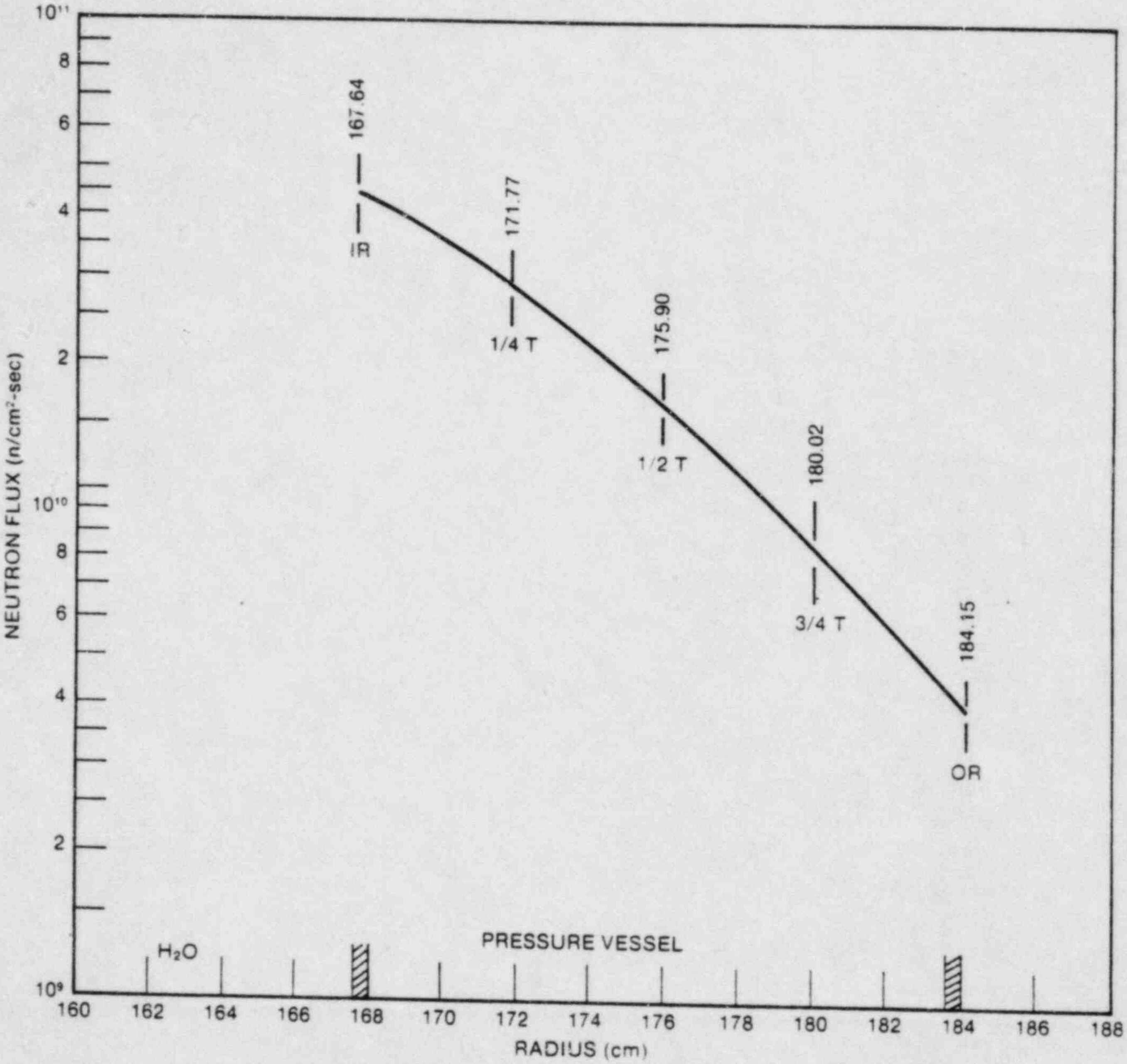

Figure 6-4. Calculated Radial Distribution of Maximum Fast Neutron Flux (E > 1.0 Mev) within the Pressure Vessel

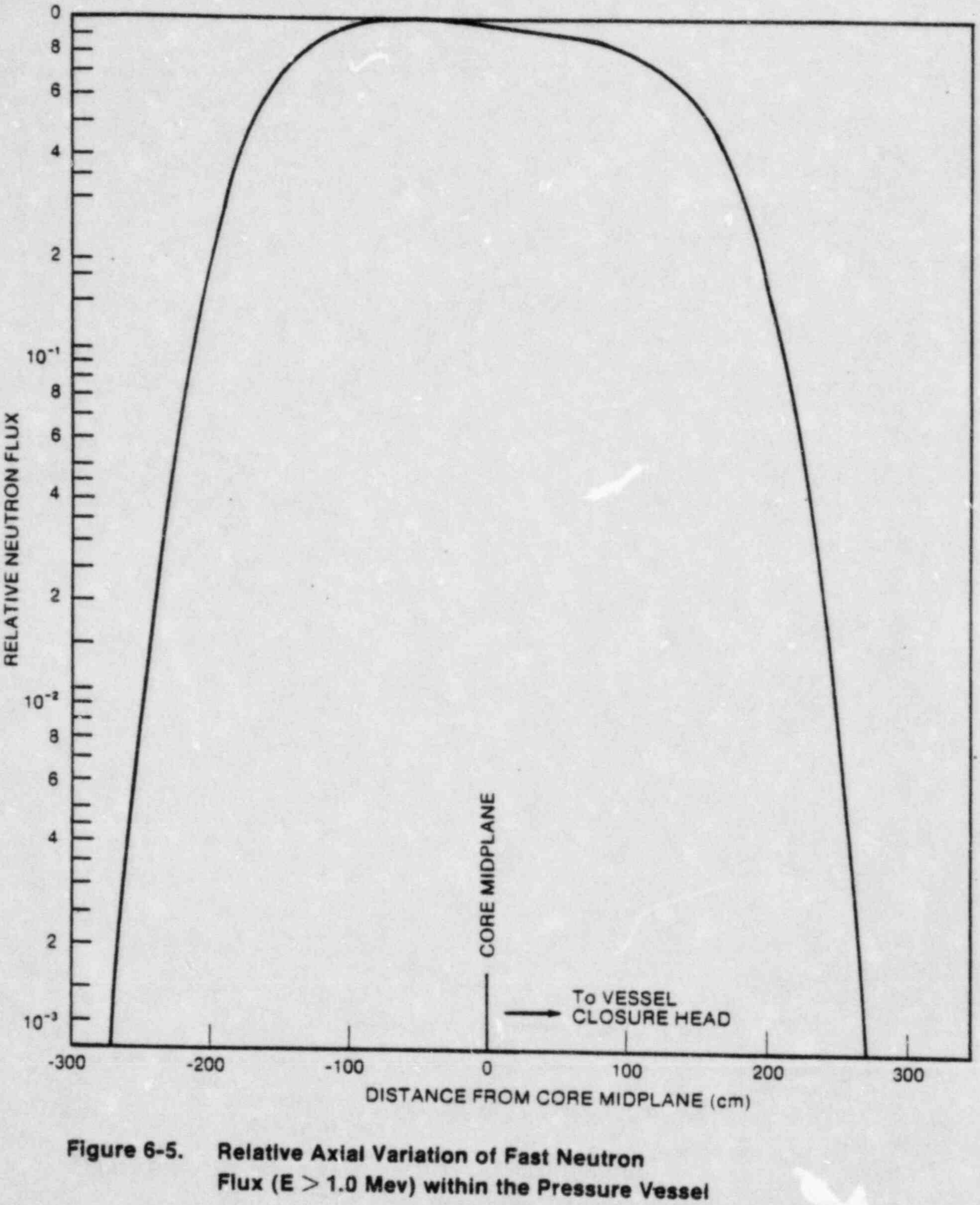

Figure 6-5. Relative Axial Variation of Fast Neutron Flux (E > 1.0 Mev) within the Pressure Vessel

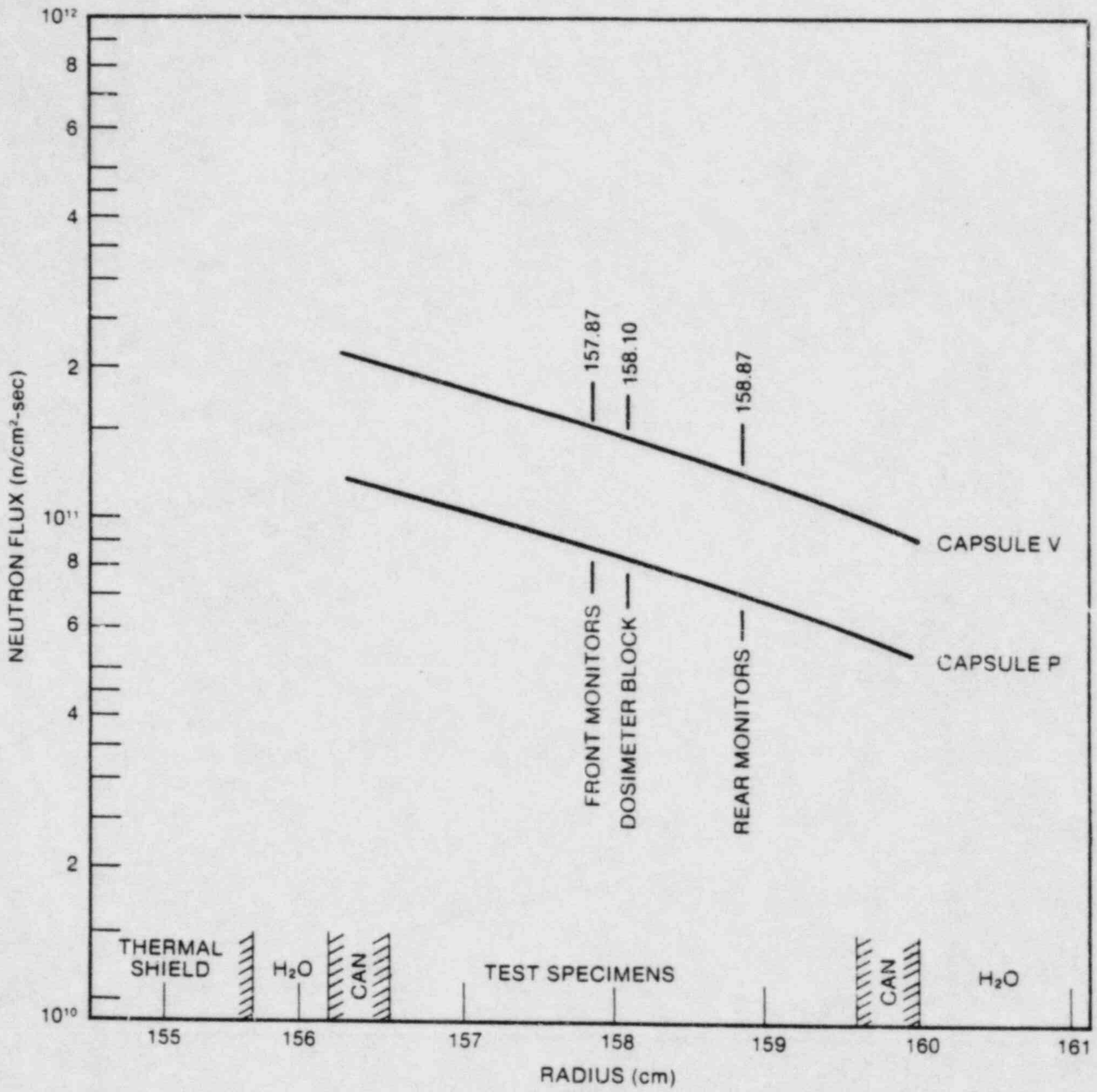

Figure 6-6. **Calculated Radial Distribution of Maximum Fast Neutron Flux (E > 1.0 Mev) within Surveillance Capsules P and V**

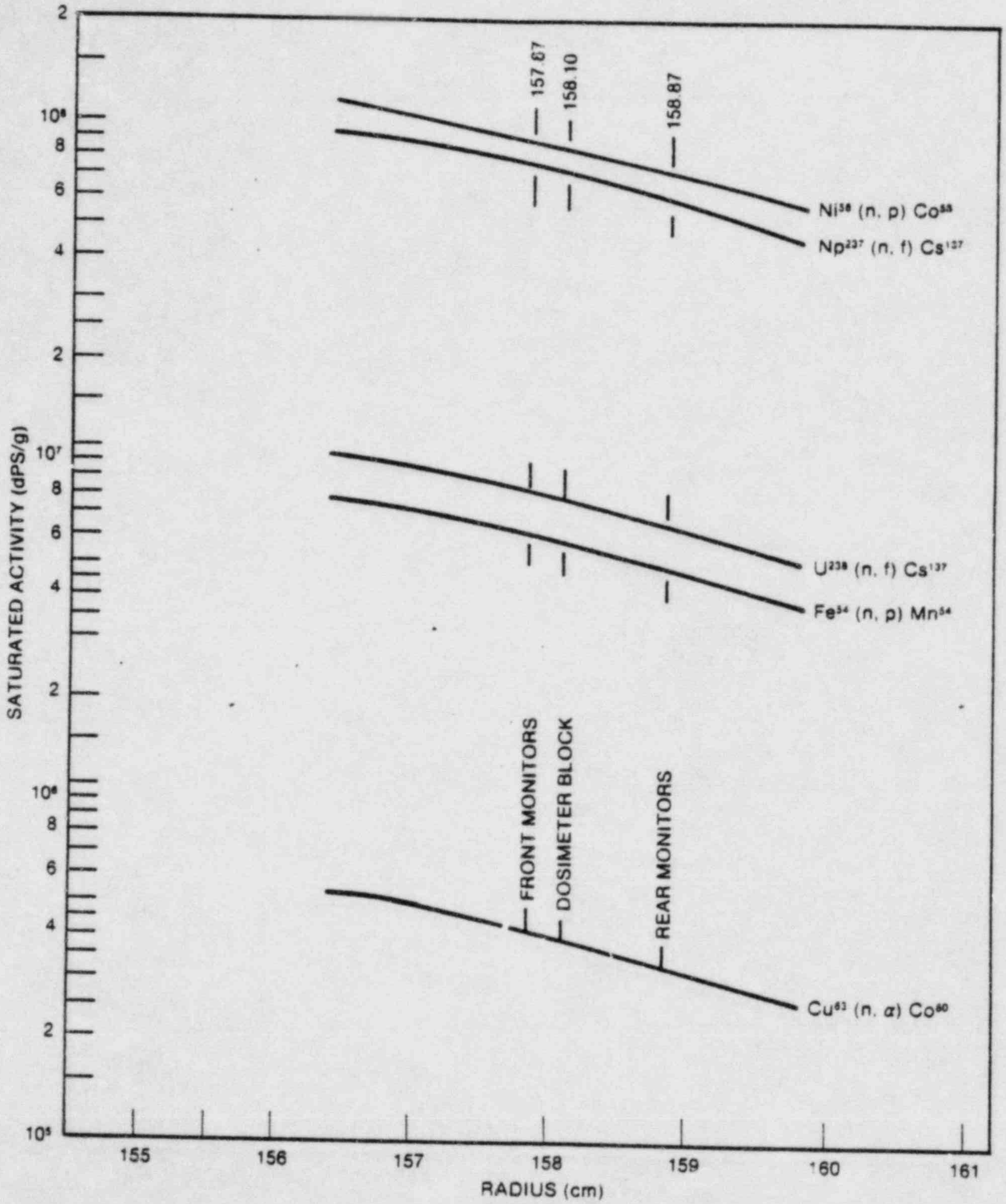

Figure 6-7. **Calculated Variation of Fast Neutron Flux Monitor Saturated Activity within Capsule V**

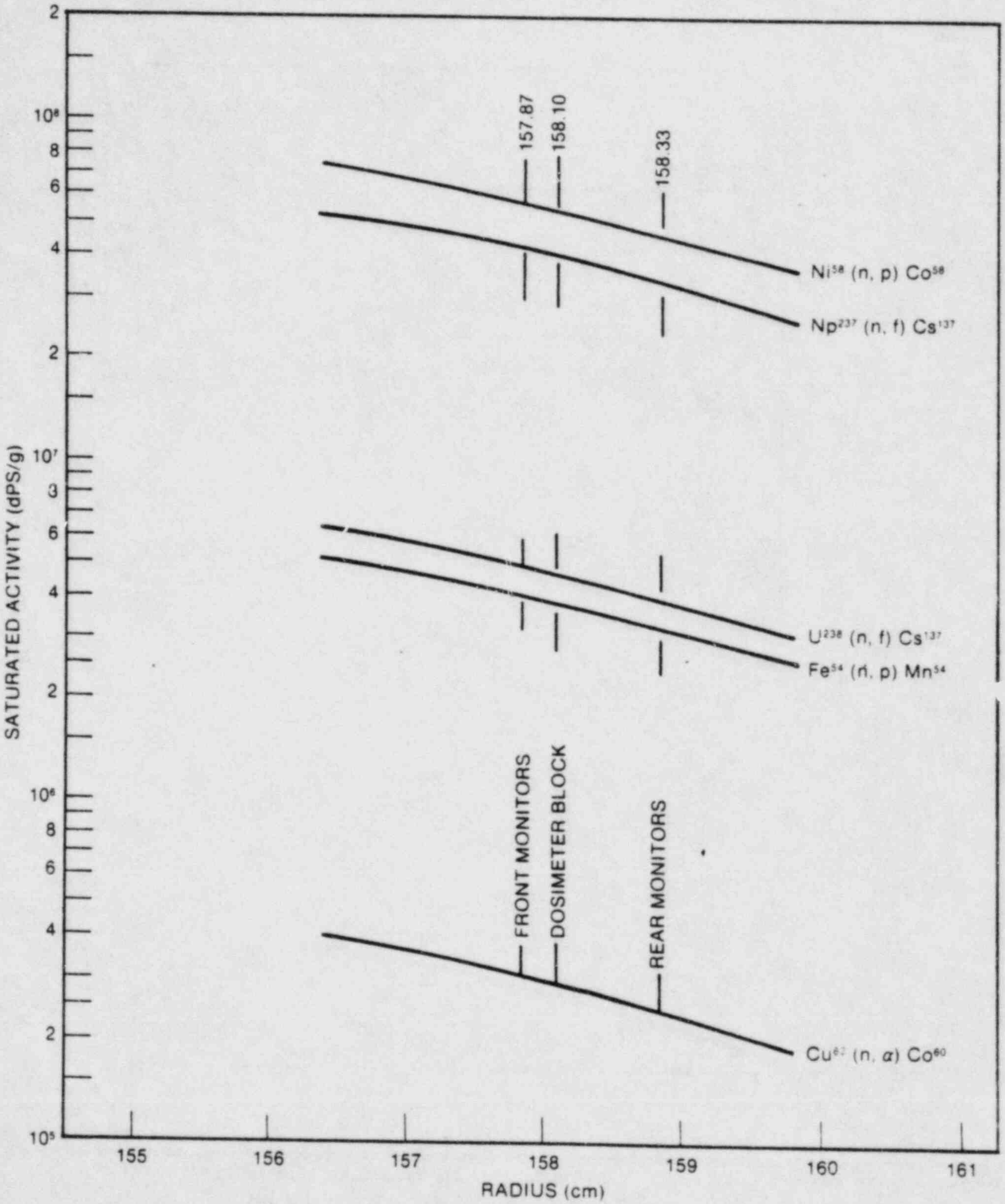

Figure 6-8. Calculated Variation of Fast Neutron Flux Monitor Saturated Activity within Capsule P

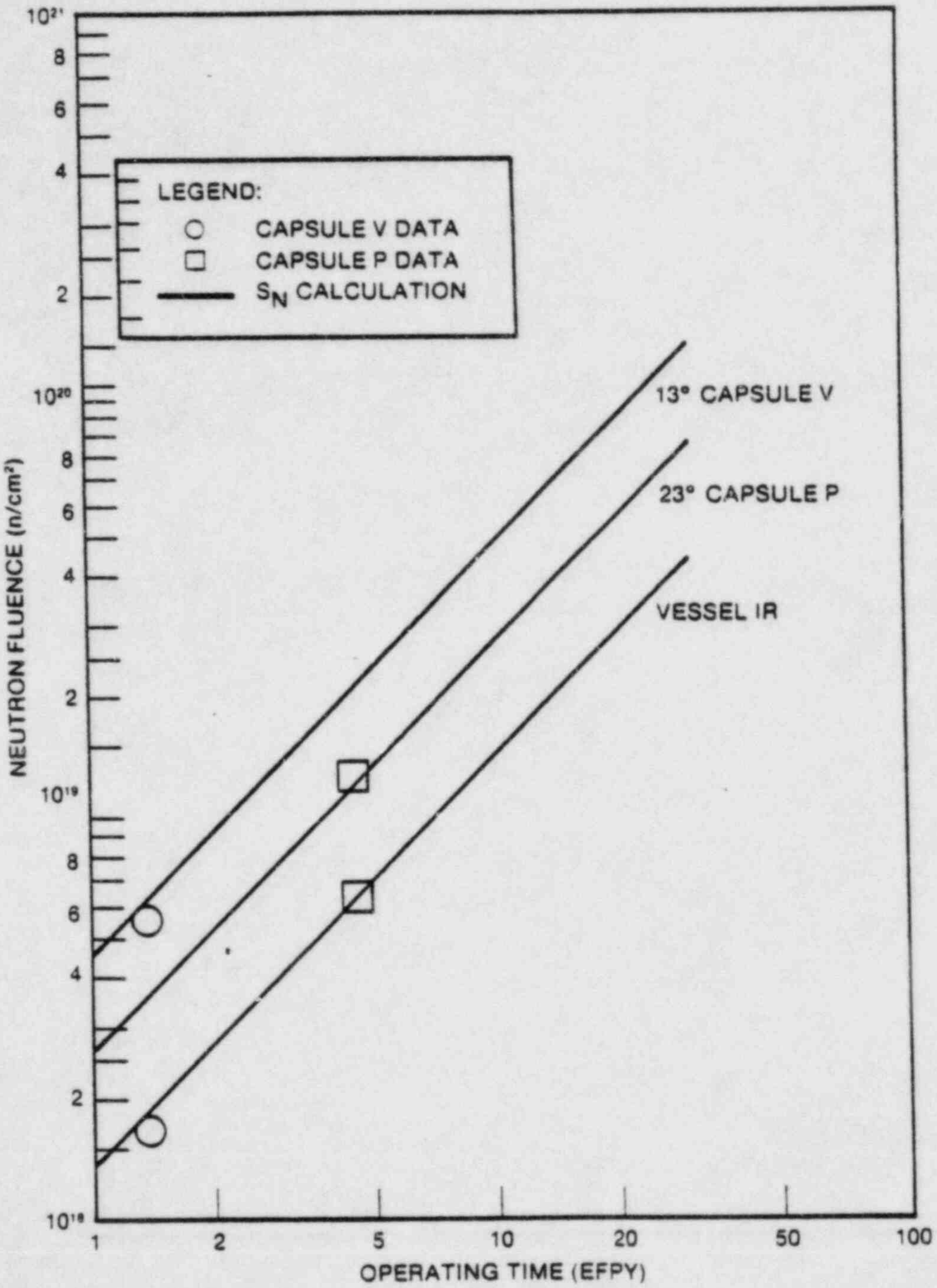

Figure 6-9. **Comparison of Measured and Calculated Fast Neutron Fluence (E > 1.0 Mev) for Capsules P and V**

SECTION 7
REFERENCES

1. Yanichko, S. E., Lege, D. J., "Northern States Power Company Prairie Island Unit No. 1 Reactor Reactor Vessel Radiation Surveillance Program," WCAP-8086, June 1973.

2. ASTM Designation E-185-73, "Surveillance Tests for Nuclear Reactor Vessels" in ASTM Standards (1974), Part 10, pp. 314-320, Am. Soc. for Testing and Materials, Philadelphia, Pa., 1974.

3. Davidson, J. A., Anderson, S. L. and Scott, K. V., "Analysis of Capsule V from Northern States Power Company Prairie Island Unit No. 1 Reactor Vessel Radiation Surveillance Program," WCAP-8916, August 1977.

4. U.S. Nuclear Regulatory Commission, Office of Nuclear Reactor Regulation, Standard Review Plan, NUREG-75/087, Sect. 5.3.2, "Pressure-Temperature Limits," November 1975.

5. Soltesz, R. G., Disney, R. K., Jedruch, J. and Ziegler, S. L., "Nuclear Rocket Shielding Methods, Modification, Updating and Input Data Preparation, Volume 5 — Two-Dimension Discrete Ordinates Transport Technique," WANL-PR(LL)034, Volume 5, August 1970.

6. Collier, G., et. al., "Second Version of the GAMB1T Code," WANL-TME-1969, November 1979.

7. Soltesz, R. G., et. al., "Nuclear Rocket Shielding Methods, Modification, Updating and Input Data Preparation — Volume 3, Cross-Section Generation and Data Processing Techniques," WANL-PR(LL)034, August 1970.

8. Soltesz, R. G., et. al., "Nuclear Rocket Shielding Methods, Modification, Updating and Input Data Preparation — Volume 4 — One-Dimensional Discrete Ordinates Transport Technique," WANL-PR(LL)034, August 1970.

9. ASTM Designation E261-70, "Standard Method for Measuring Neutron Flux by Radioactivation Techniques," in ASTM Standards (1975), Part 45, Nuclear Standards, pp. 745-755, Am. Society for Testing and Materials, Philadelphia, Pa., 1975.

10. ASTM Designation E262-70, "Standard Method for Measuring Thermal Neutron Flux by Radioactivation Techniques," in ASTM Standards (1975), Part 45, Nuclear Standards, pp. 756-763, Am. Society for Testing and Materials, Philadelphia, Pa., 1975.

11. ASTM Designation E263-70, "Standard Method for Measuring Fast-Neutron Flux by Radioactivation of Iron," in ASTM Standards (1975), Part 45, Nuclear Standards, pp. 764-769, Am. Society for Testing and Materials, Philadelphia, Pa., 1975.

12. ASTM Designation E481-73T, "Tentative Method of Measuring Neutron-Flux Density by Radioactivation of Cobalt and Silver," in ASTM Standards (1975), Part 45, Nuclear Standards, pp. 887-894, Am. Society for Testing and Materials, Philadelphia, Pa., 1975.

13. ASTM Designation E264-70, "Standard Method for Measuring Fast-Neutron Flux by Radioactivation of Nickel," in ASTM Standards (1975), Part 45, Nuclear Standards, pp. 770-774, Am. Society for Testing and Materials, Philadelphia, Pa., 1975.

APPENDIX A

HEATUP AND COOLDOWN LIMIT CURVES FOR NORMAL OPERATION

A-1. INTRODUCTION

Heatup and cooldown limit curves are calculated using the most limiting value of RT_{NDT} (reference nil-ductility temperature). The most limiting RT_{NDT} of the material in the core region of the reactor vessel is determined by using the preservice reactor vessel material properties and estimating the radiation-induced ΔRT_{NDT}. RT_{NDT} is designated as the higher of either the drop weight nil-ductility transition temperature (T_{NDT}) or the temperature at which the material exhibits at least 50 ft lb of impact energy and 35-mil lateral expansion (normal to the major working direction) minus 60°F.

RT_{NDT} increases as the material is exposed to fast-neutron radiation. Thus, to find the most limiting RT_{NDT} at any time period in the reactor's life, ΔRT_{NDT} due to the radiation exposure associated with that time period must be added to the original unirradiated RT_{NDT}. The extent of the shift in RT_{NDT} is enhanced by certain chemical elements (such as copper and phosphorus) present in reactor vessel steels. The Regulatory Guide 1.99 trend curves which show the effect of fluence and copper and phosphorus contents on ΔRT_{NDT} for reactor vessel steels are shown in Figure A-1.

Given the copper and phosphorus contents of the most limiting material, the radiation-induced ΔRT_{NDT} can be estimated from Figure A-1. Fast-neutron fluence ($E > 1$ Mev) at the 1/4 T (wall thickness) and 3/4 T (wall thickness) vessel locations are given as a function of full-power service life in Figure A-2. The data for all other ferritic materials in the reactor coolant pressure boundary are examined to insure that no other component will be limiting with respect to RT_{NDT}.

A-2. FRACTURE TOUGHNESS PROPERTIES

The preirradiation fracture-toughness properties of the Prairie Island Unit 1 reactor vessel materials are presented in Table A-1. The fracture toughness properties of the ferritic material in the reactor coolant pressure boundary are determined in accordance with the NRC Regulatory Standard Review Plan.[1] The postirradiation fracture

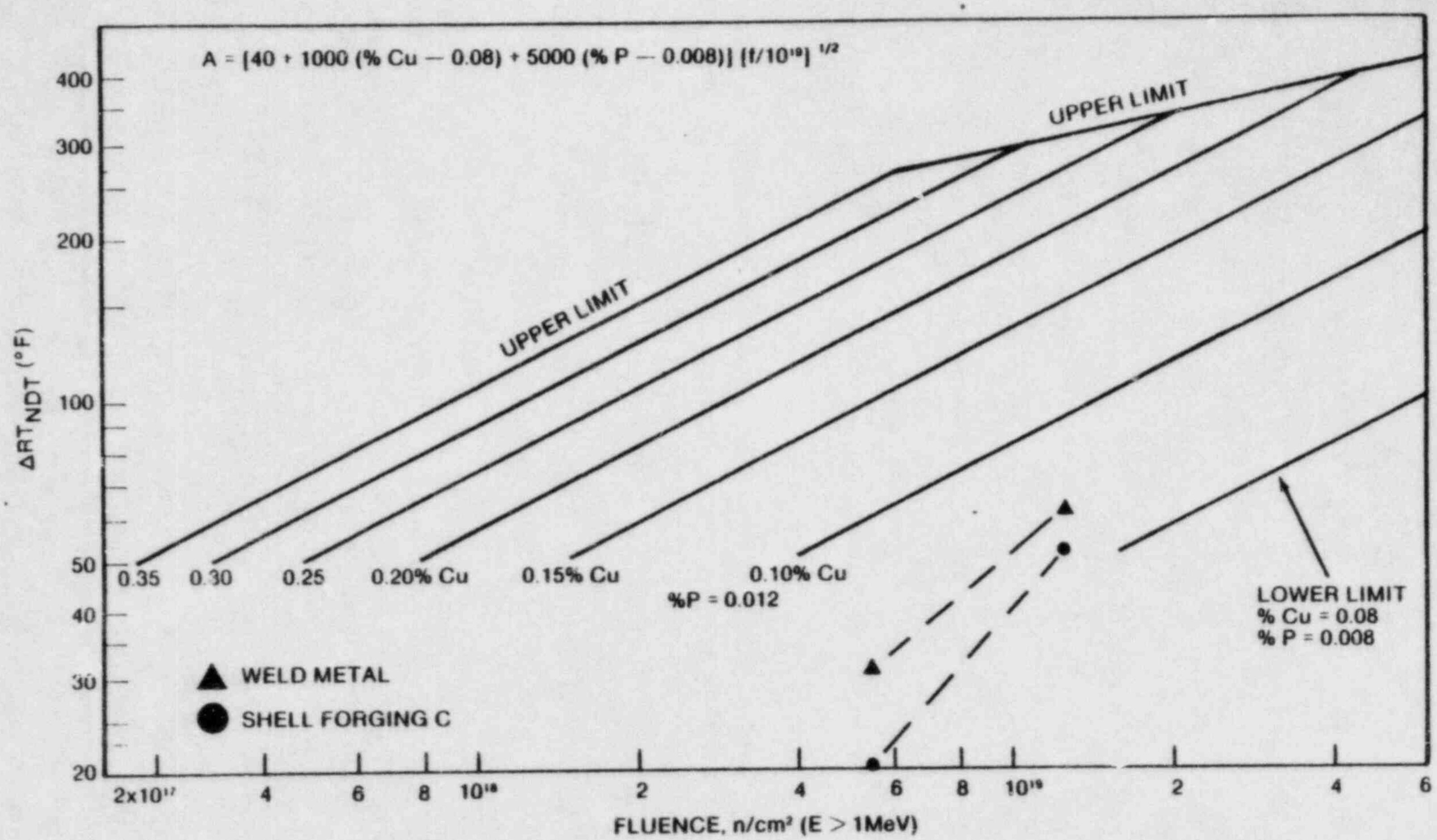

Figure A-1. Effect of Fluence, Copper Content, and Phosphorus Content on ΔRT_{NDT} for Reactor Vessel Steels per Regulatory Guide 1.99

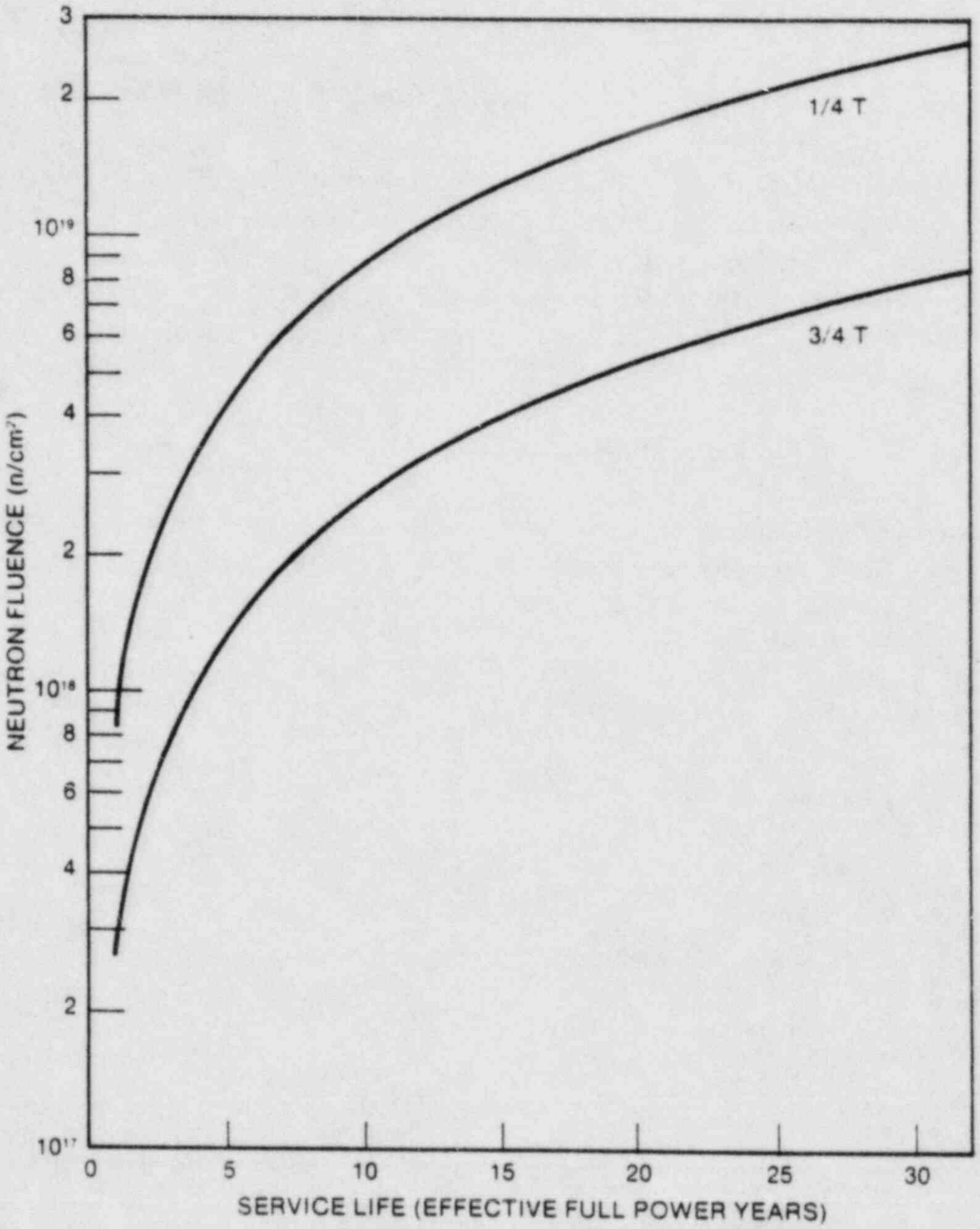

Figure A-2. Fast Neutron Fluence (E > 1.0 Mev) as a Function of Full Power Service Life

toughness properties of the reactor vessel beltline material were obtained directly from the Prairie Island Unit 1 Vessel Material Surveillance Program.

A-3. CRITERIA FOR ALLOWABLE PRESSURE-TEMPERATURE RELATIONSHIPS

The ASME approach for calculating the allowable limit curves for various heatup and cooldown rates specifies that the total stress intensity factor, K_I, for the combined thermal and pressure stresses at any time during heatup and cooldown cannot be greater than the reference stress intensity factor, K_{IR}, for the metal temperature at that time. K_{IR} is obtained from the reference fracture toughness curve, defined in Appendix G to the ASME Code.[2] The K_{IR} curve is given by the equation:

$$K_{IR} = 26.78 + 1.223 \exp [0.0145 (T-RT_{NDT} + 160)] \quad \text{(A-1)}$$

where K_{IR} is the reference stress intensity factor as a function of the metal temperature T and the metal reference nil-ductility temperature RT_{NDT}. Thus, the governing equation for the heatup-cooldown analysis is defined in Appendix G to the ASME Code[2] as follows:

$$C K_{IM} + K_{It} \leq K_{IR} \quad \text{(A-2)}$$

TABLE A-1

REACTOR VESSEL TOUGHNESS DATA (UNIRRADIATED)

Component	Material Type	Cu (%)	P (%)	NDTT (°F)	NMWD 50 ft lb/35 mils Lateral Expansion Temperature (°F)	RT_{NDT} (°F)	NMWD Upper Shelf Energy (ft lb)
Closure Head Dome	A533 Gr. B, Cl. 1			-4	64[a]	4[a]	75[a]
Head Flange	A508 Cl. 3			-4	12[a]	-4[a]	84[a]
Vessel Flange	A508 Cl. 3			-4	41[a]	-4[a]	77.5[a]
Injection Nozzles	A508 Cl. 3			-22	-114[a]	-22[a]	97[a]
Inlet and Outlet Nozzle	A508 Cl. 3			+5	39[a]	5[a]	92[a]
Upper Shell	A508 Cl. 3			-4	39[a]	-4[a]	85[a]
Inter. Shell	A508 Cl. 3	0.06	0.013	+14	14	14	143
Lower Shell	A508 Cl. 3	0.07	0.014	-4	45	-4	134
Trans. Ring	A508 Cl. 3			+5	63[a]	5[a]	79[a]
Bottom Head	A533 Gr. B, Cl. 1			-4	57[a]	-3[a]	68.5[a]
Inter. to Lower Shell Girth Weld	Sub-Arc Weld	0.13	0.017	0	10	0	78.5
Weld HAZ	HAZ			0[a]	<-100	0	211

a. Estimated using the NRC Standard Review Plan.

where

K_{IM} is the stress intensity factor caused by membrane (pressure) stress

K_{It} is the stress intensity factor caused by the thermal gradients

K_{IR} is a function of temperature to the RT_{NDT} of the material

C = 2.0 for Level A and Level B service limits

C = 1.5 for hydrostatic and leak test conditions during which the reactor core is not critical

At any time during the heatup or cooldown transient, K_{IR} is determined by the metal temperature at the tip of the postulated flaw, the appropriate value for RT_{NDT}, and the reference fracture toughness curve. The thermal stresses resulting from temperature gradients through the vessel wall are calculated and then the corresponding (thermal) stress intensity factors, K_{It}, for the reference flaw are computed. From equation (A-2), the pressure stress intensity factors are obtained and, from these, the allowable pressures are calculated.

For the calculation of the allowable pressure-versus-coolant temperature during cooldown, the Code reference flaw is assumed to exist at the inside of the vessel wall. During cooldown, the controlling location of the flaw is always at the inside of the wall because the thermal gradients produce tensile stresses at the inside, which increase with increasing cooldown rates. Allowable pressure-temperature relations are generated for both steady-state and finite cooldown rate situations. From these relations, composite limit curves are constructed for each cooldown rate of interest.

The use of the composite curve in the cooldown analysis is necessary because control of the cooldown procedure is based on measurement of reactor coolant temperature, whereas the limiting pressure is actually dependent on the material temperature at the tip of the assumed flaw. During cooldown, the 1/4 T vessel location is at a higher temperature than the fluid adjacent to the vessel ID. This condition, of course, is not true for the steady-state situation. It follows that, at any given reactor coolant temperature, the ΔT developed during cooldown results in a higher value of K_{IR} at the 1/4 T location for finite cooldown rates than for steady-state operation.

Furthermore, if conditions exist such that the increase in K_{IR} exceeds K_{It}, the calculated allowable pressure during cooldown will be greater than the steady-state value.

The above procedures are needed because there is no direct control on temperature at the 1/4 T location and, therefore, allowable pressures may unknowingly be violated if the rate of cooling is decreased at various intervals along a cooldown ramp. The use of the composite curve eliminates this problem and insures conservative operation of the system for the entire cooldown period.

Three separate calculations are required to determine the limit curves for finite heatup rates. As is done in the cooldown analysis, allowable pressure-temperature relationships are developed for steady-state conditions as well as finite heatup rate conditions assuming the presence of a 1/4 T defect at the inside of the vessel wall. The thermal gradients during heatup produce compressive stresses at the inside of the wall that alleviate the tensile stresses produced by internal pressure. The metal temperature at the crack tip lags the coolant temperature; therefore, the K_{IR} for the 1/4 T crack during heatup is lower than the K_{IR} for the 1/4 T crack during steady-state conditions at the same coolant temperature. During heatup, especially at the end of the transient, conditions may exist such that the effects of compressive thermal stresses and lower K_{IR}'s do not offset each other, and the pressure-temperature curve based on steady-state conditions no longer represents a lower bound of all similar curves for finite heatup rates when the 1/4 T flaw is considered. Therefore, both cases have to be analyzed in order to insure that at any coolant temperature the lower value of the allowable pressure calculated for steady-state and finite heatup rates is obtained.

The second portion of the heatup analysis concerns the calculation of pressure-temperature limitations for the case in which a 1/4 T deep outside surface flaw is assumed. Unlike the situation at the vessel inside surface, the thermal gradients established at the outside surface during heatup produce stresses which are tensile in nature and thus tend to reinforce any pressure stresses present. These thermal stresses are dependent on both the rate of heatup and the time (or coolant temperature) along the heatup ramp. Since the thermal stresses at the outside are tensile and increase with increasing heatup rates, each heatup rate must be analyzed on an individual basis.

Following the generation of pressure-temperature curves for both the steady-state and finite heatup rate situations, the final limit curves are produced as follows: A composite curve is constructed based on a point-by-point comparison of the steady-state and finite heatup rate data. At any given temperature, the allowable pressure is taken to be the lesser of the three values taken from the curves under consideration. The use of the composite curve is necessary to set conservative heatup limitations because it is possible for conditions to exist wherein, over the course of the heatup ramp, the controlling condition switches from the inside to the outside and the pressure limit must at all times be based on analysis of the most critical criterion. Then, composite curves for the heatup rate data and the cooldown rate data are adjusted for possible errors in the pressure and temperature sensing instruments by the values indicated on the respective curves.

A-4. HEATUP AND COOLDOWN LIMIT CURVES

Limit curves for normal heatup and cooldown of the primary Reactor Coolant System have been calculated using the methods discussed in paragraph A-3. The derivation of the limit curves is presented in the NRC Regulatory Standard Review Plan.[3]

Transition temperature shifts occurring in the pressure vessel materials due to radiation exposure have been obtained directly from the reactor pressure vessel surveillance program.

Charpy test specimens from Capsule P irradiated to 1.25×10^{19} n/cm^2 indicate that the core region weld metal and the limiting core region shell forging C exhibited maximum shifts in RT_{NDT} of 60° F, respectively as shown by Figure A-1. The shifts are well within the appropriate design curve (Figure A-1) prediction. Heatup and cooldown limit curves for normal operation of Prairie Island Unit 2 for up to 20 effective-full-power years (EFPY) were presented in the Capsule radiation surveillance program report.[4] These heatup and cooldown curves are applicable for Prairie Island Unit 1 up to 7.4 EFPY, and they are shown in Figures A-3 and A-4.

Allowable combinations of temperature and pressure for specific temperature change rates are below and to the right of the limit lines shown on the heatup and cooldown curves. The reactor must not be made critical until pressure-temperature combinations are to the right of the criticality limit line, shown in Figure A-3. This is in addition to other criteria which must be met before the reactor is made critical.

The leak test limit curve shown in Figure A-3 represents minimum temperature requirements at the leak test pressure specified by applicable codes. The leak test limit curve was determined by methods of reference.[2,5]

Figures A-3 and A-4 define limits for insuring prevention of nonductile failure.

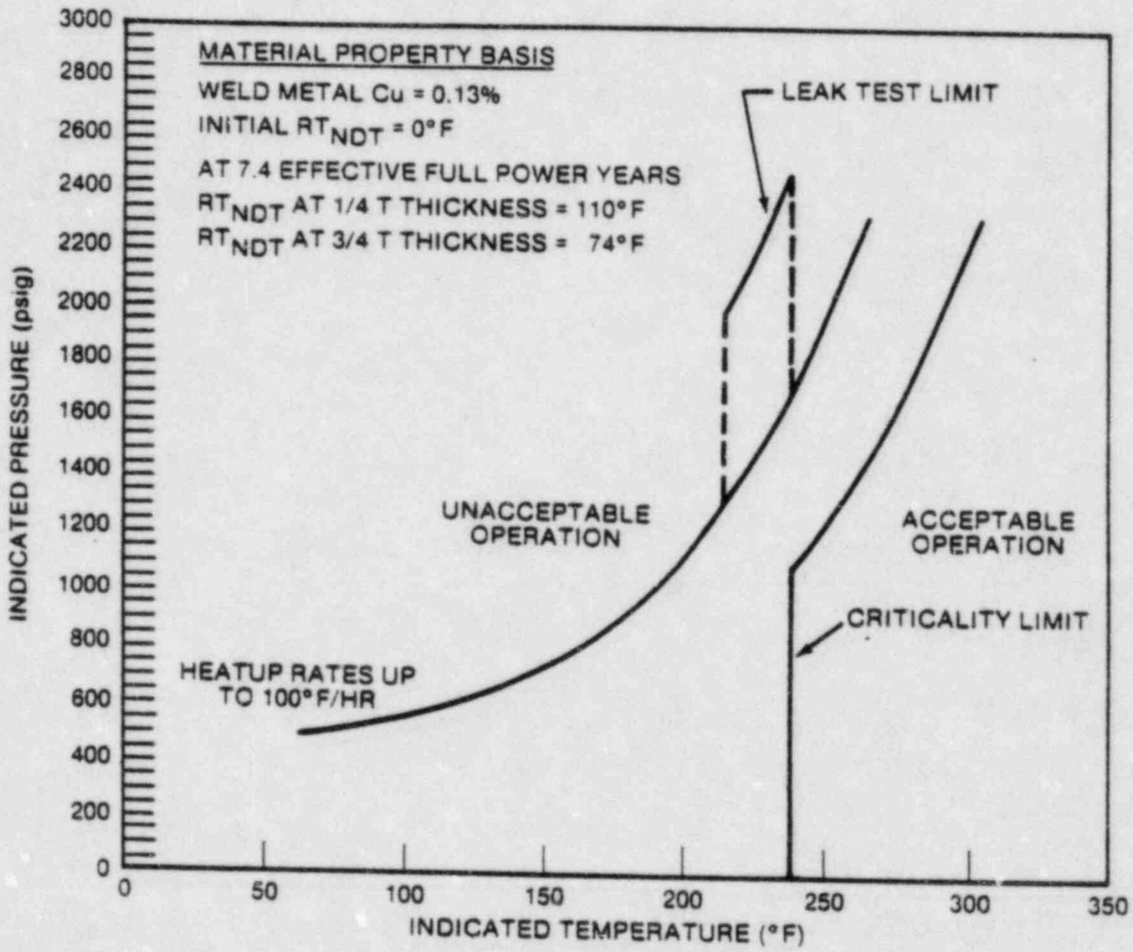

Figure A-3. Prairie Island Unit 1 Reactor Coolant System Heatup Limitations Applicable for Periods up to 7.4 Effective Full Power Years. Margins of 60 psig and 10°F are Included for Possible Instrument Error

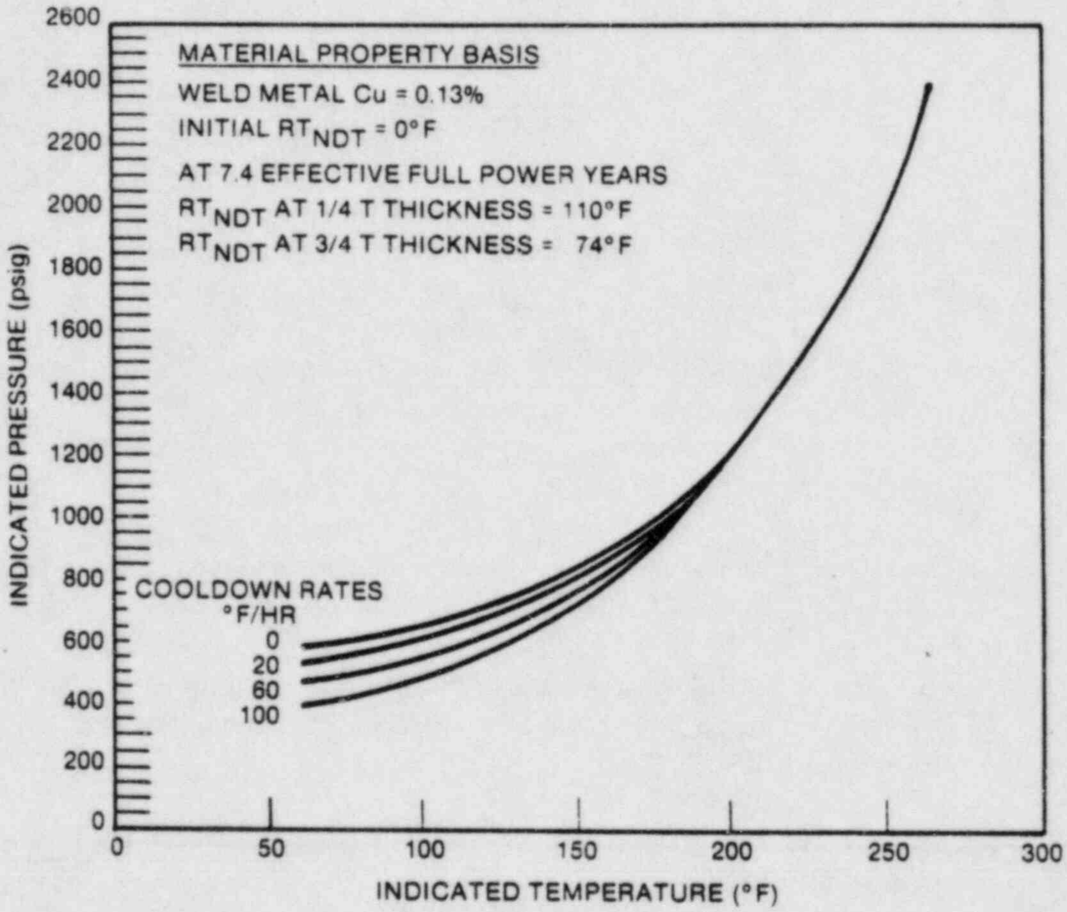

Figure A-4. **Prairie Island Unit 1 Reactor Coolant System Cooldown Limitations Applicable for Periods up to 7.4 Effective Full Power Years. Margins of 60 psig and 10°F are Included for Possible Instrument Error**

APPENDIX A
REFERENCES

1. "Fracture Toughness Requirements," Branch Technical Position MTEB No. 5-2, Section 5.3.2-14 in Standard Review Plan, NUREG-75/087, 1975.

2. ASME Boiler and Pressure Vessel Code, Section III, Division 1 — Appendices, "Rules for Construction of Nuclear Vessels," Appendix G, "Protection Against Nonductile Failure," pp. 461-469, 1980 Edition, American Society of Mechanical Engineers, New York, 1980.

3. "Pressure-Temperature Limits," Section 5.3.2 in Standard Review Plan, NUREG-75/987, 1975.

4. Yanichko, S. E., and Anderson, S. L., "Analysis of Capsule T from Northern States Power Company Prairie Island Unit No. 2 Reactor Vessel Radiation Surveillance Program," WCAP-9877, March 1981.

5. "Pressure-Temperature Limits," Section 5.3.2 in Standard Review Plan, NUREG-75/087, 1975.